Teleconnections between the northern North Atlantic and the Tropical Atlantic

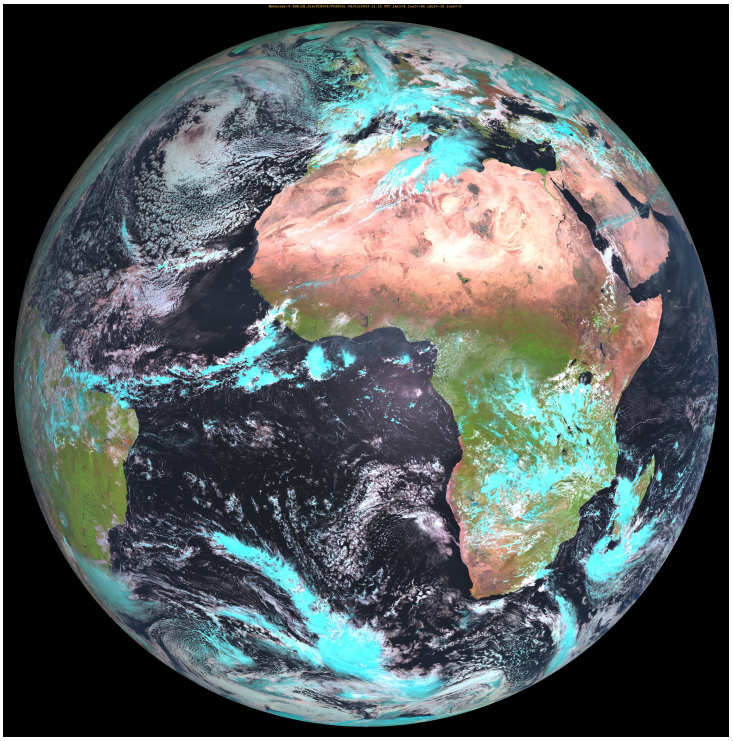

Márcia Luiza Pearson
Erasmus Mundus Joint Master in
Water and Coastal Management

Supervisor: Tore Furevik
Geophysical Institute, University of Bergen – Norway
April 2009

Written in LaTeX 2ε, 11 point text, report style and twosided format. Edited with TeXShop and BibDesk.

Image in the front page: Cloud cover in the Atlantic sector. The ITCZ is visible in the center, close to its southernmost position. Image from Meteosat Second Generation, MSG–2, 4^{th} of March 2009. Kindly provided by Humberto Barbosa (EUMETCast, Laboratório de Processamento de Imagens de Satélites – LAPIS, Instituto de Ciências Atmosféricas, Universidade Federal de Alagoas, Brazil).

Acknowledgements

First of all, I wish to thank to my supervisor Tore Furevik for the helpful discussions, comments and support during the work on this thesis. To Prof. Eystein Jansen, director of the Bjerknes Centre for Climate Research for providing the paleoclimatic reconstruction that motivated the choice of subject. I am pleased to have attended Øyvind Breivik's data analysis course and I wish to thank him for his help with the EOFs. I am immensely thankful to the Erasmus Mundus program for the scholarship received and the opportunity to study in Europe. I appreciate all the time that Carmen López and Ángel del Valls Casillas, from University of Cádiz, Rune Rosland, Berit Øglænd and Sidsel Kjølleberg, from Bergen University, spent caring for all the bureaucratic details that made this possible. I am grateful to Humberto Barbosa, André Vitta, Kurt Vildgren and to my brazilian "Little Ice Age" - Lia Jacobsen, for their friendly and valuable help. I am happy to have shared the "dark cave" with Christine, Ahmed, Elfatih, Salma, Waleed, Pelle and all the Mozambique students at the Geophysics Institute during this long lasting semester. Maybe we see each other some day again and "go to the pub" together! Lastly I am grateful for all the remote positive thoughts from friends and family sent from Brazil, Spain, Portugal, Ireland, Germany and Thailand. I've tried to capture them all, but even warm signals loose strength, specially when traveling all the way north to the cold higher latitudes. Many others have helped in different ways, and even though they might never know they did, I am deeply thankful.

Abstract

Paleoclimatic reconstructions of variations in rainfall and upwelling in the tropical Cariaco Basin, off Venezuela coast, suggest that meridional displacement of the Intertropical Convergence Zone (ITCZ) is linked to high latitude sea surface temperature (SST) anomalies at different timescales. This study investigates instrumental records in search for covariability between the Cariaco Basin area and the Norwegian Sea. The interannual correlation between the Norwegian Sea SST anomalies and SST elsewhere are similar to the North Atlantic Oscillation (NAO) imprint on the SST in the North Atlantic. This indicates that at these timescales the NAO's atmospheric forcing dominates the air-sea interactions over the North Atlantic. However, they can not fully explain the weak interannual correlations between the SST and sea level pressure (SLP) indices of the Norwegian and Caribbean Seas. At interdecadal timescales the whole Atlantic seems to be dominated by a basin wide spatial pattern of positive correlations, which roughly resembles the Atlantic Multidecadal Oscillation (AMO) spatial pattern. This is believed to describe variations of the thermohaline circulation (THC). The resulting pattern of the Norwegian Sea SST correlated with the SLP elsewhere, both at interannual and interdecadal timescales, is similar to the anomalous SST conditions in the North Atlantic associated with a dipole-like atmospheric circulation, that modifies the air-sea interactions and the THC intensity. Despite some discrepancies with other studies, our results indicate that the interdecadal covariability between the Norwegian and the Caribbean Seas is due to the existence of the THC, and that its strength is modulated by the wind-evaporation mechanism, local processes or remote forcing through an atmospheric teleconnection.

Contents

Chapter 1

Introduction

Although climate variability and climate change are now better understood than ever, still many climate processes (both atmospheric and oceanic) are not fully understood. The way different climate components behave and interact among each other, through teleconnection patterns and distant climatic linkages for example, is one of them. The interest in teleconnections dynamics and their social and economic impacts increased after the intense El Niño events of 1982-83 and 1997-98. The aftermath associated with these events, included losses in agriculture and fisheries, floods and droughts, and consequent famines in different regions worldwide (Glantz et al., 1991, chapters 13-16).

Teleconnections are usually defined as the link between climate anomalies at one place and climate anomalies at a distant location, and can modify weather patterns over great distances and timescales. Both the atmosphere and the ocean can act as "bridges" or "tunnels" creating patterns of teleconnections mainly through the transport of energy (heat) or momentum (wave propagation). Atmospheric teleconnections are fast and typically associated with Rossby wave propagation, that allows maximum teleconnectivity to be reached within the scale of few days. In contrast, oceanic driven connections depend on circulation processes, and therefore are involved in very low frequency climate variability (typically decades to millennium). Linkages can happen in meridional and zonal directions, leading climatic events to be connected between regions in the tropics and extratropics, between middle and high latitudes, or even between hemispheres. The main ways of interactions between atmospheric and oceanic teleconnections are illustrated in Fig. 1.1 (Liu & Alexander, 2007).

Atmospheric teleconnections can be forced both by internal variability of the atmosphere or by boundary conditions, such as sea surface temperature (SST) anomalies (Liu & Alexander, 2007). A clear example for the first case is the North Atlantic Oscillation (NAO), which reflects the interaction between the internal dynamics of the atmosphere with storm tracks, mainly during the Northern Hemisphere winter (Marshall et al., 2001), which greatly affect precipitation and air temperature patterns over Europe. The El Niño Southern Oscillation (ENSO) is a good example of how an air-sea interaction works, with atmospheric responses primarily driven by anomalous warming of SST in the Equatorial Pacific Ocean and the Peruvian coast, with effects spread worldwide through teleconnection patterns (Glantz et al., 1991).

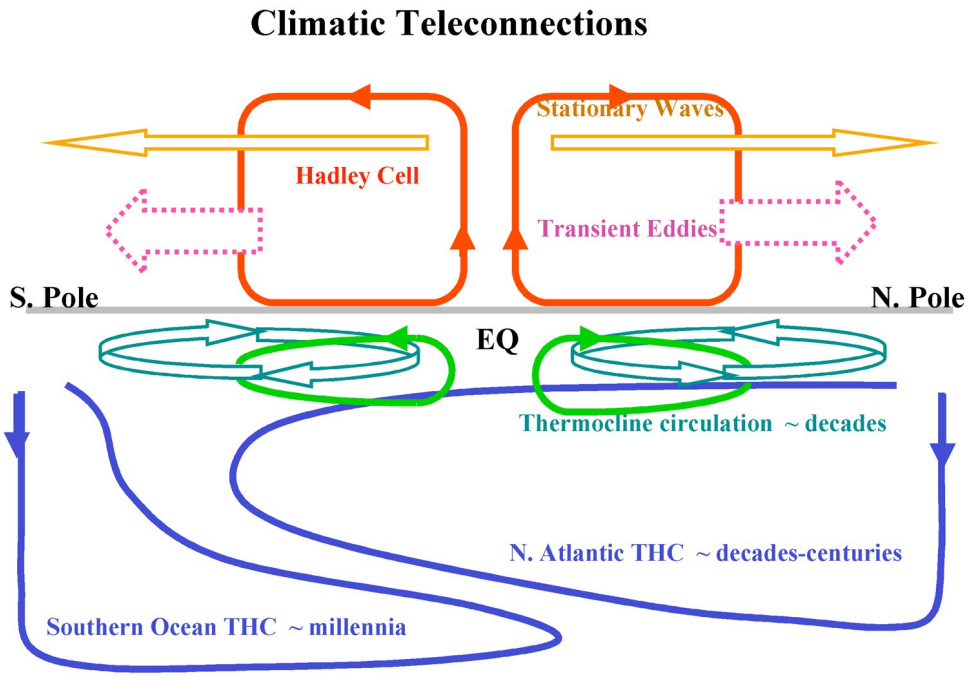

Figure 1.1: Main directions of teleconnections. Atmospheric branches are faster, and anomalies in the mean circulation are transmitted through changes in intensity and location of atmospheric cells or their centers, Rossby waves and storm tracks. Oceanic linkages have longer timescales, and involve subduction processes in the oceans, due to changes in heat and freshwater fluxes. At the same time air-sea interactions connect both fluids. From Liu & Alexander (2007); their Figure 5.

In the North Atlantic three main mechanisms account for the major part of the climate variability: the North Atlantic Oscillation (NAO), the tropical Atlantic variability (TAV), the Atlantic Meridional Circulation (MOC) (Marshall et al., 2001), and their relations with the Intertropical Convergence Zone (ITCZ). These are further reviewed in Chapter 2.

A large number of widespread paleoclimatic proxy data suggest linkages between the climate in the tropics and high northern latitudes (Fig. 1.2). Proxy records such as the sediments of Cariaco Basin, off the Venezuela coast, appear to match with proxy air temperature records of Greenland ice cores (Lea et al., 2003; Peterson & Haug, 2006). This sediment core provides a registry of interannual to century scale variability of tropical upwelling, trade winds, rainfall and ITCZ position in the Caribbean Sea. Furthermore, changes in the mean position of the ITCZ, the main process that controls the rainfall in the tropics, seem to have been synchronized with North Atlantic SST during important climatological events, such as the Little Ice Age and the Younger Dryas (Black et al., 1999; Haug et al., 2001; Peterson & Haug, 2006).

Other registers in South America, such as sediments in lake Titicaca (Baker, 2002), ice in the Bolivian Altiplano (Baker et al., 2001), pollen (Ledru et al., 2002) and speleothems (Wang et al., 2004) in the Brazilian Nordeste region complement the registers of Cariaco Basin. Their opposite positions relative to the ITCZ indicate that wetter than normal conditions occurred in these areas while the Caribbean watershed experienced drier than normal periods and intensi-

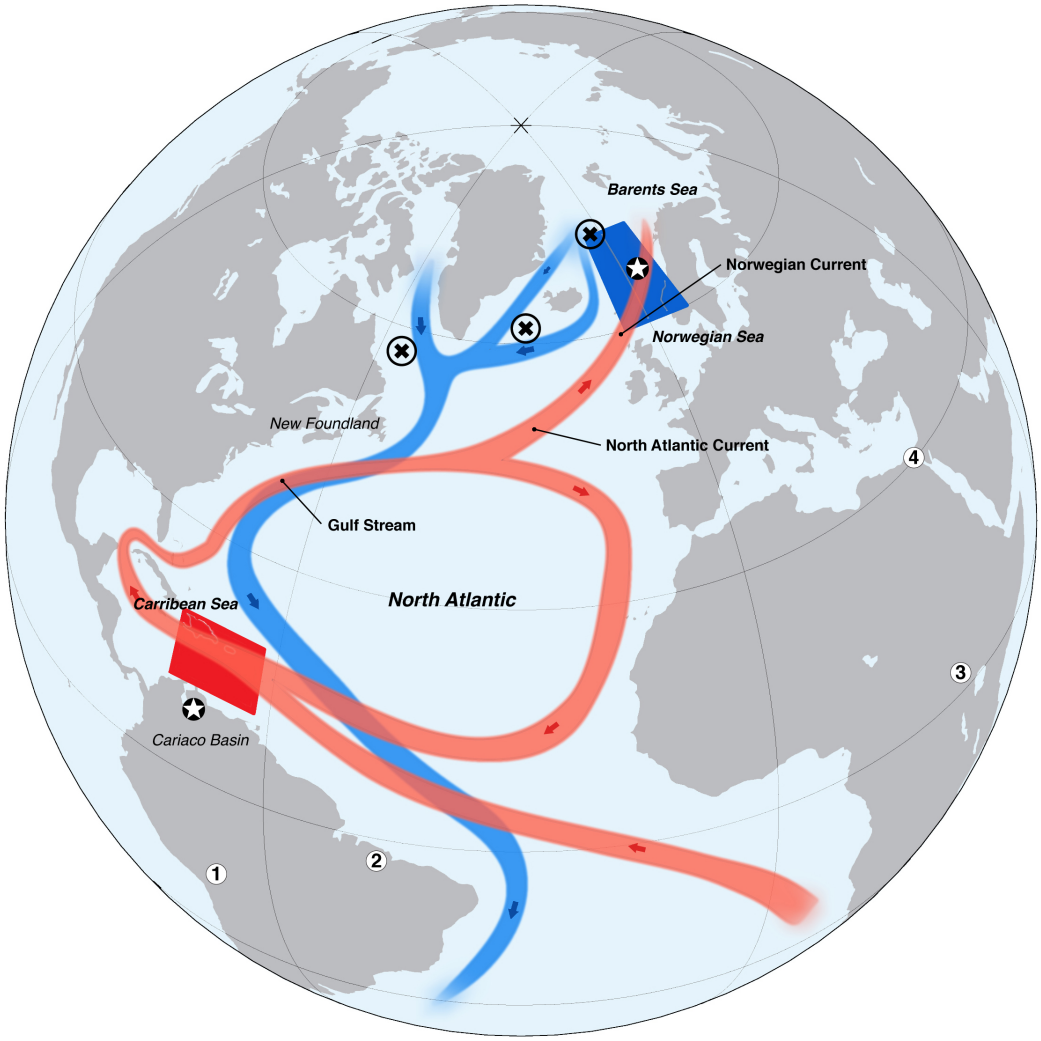

Figure 1.2: Location of most of the places mentioned in the text. Main North Atlantic currents are also shown. ⊗ represent the subsidence zones, where surface waters (red) become dense enough to sink and form deep waters, and ⋆ the location of the proxy records shown in Fig. 1.3. Numbers indicate the approximate location of other paleoclimatic reconstructions referred on the text: 1. Bolivian Altiplano, Salar de Uyunni, Volcan Sajama and Lake Titicaca; 2. brazilian Nordeste; 3. Lake Malawi and 4. Red Sea. Colored areas in the Caribbean Sea and Norwegian Sea are chosen to create mean anomaly indices for sea level pressure (SLP) and sea surface temperature (SST). The area in the tropics encloses the Cariaco Basin, where evidence of relation between the rainfall, ITCZ position, upwelling regime and high latitude SST has been found (Black et al., 1999; Peterson & Haug, 2006). The Nordic Seas along the northern extension of the Gulf Stream (red branches) is at the same time, and to a large extent, influenced by the North Atlantic current. It can therefore be connected to variations in the tropics through the Meridional Overturning Circulation (MOC, blue branches) or through changes in the atmospheric circulation (Marshall et al., 2001; Hurrell et al., 2006).

fied upwelling. The shifts in the ITCZ position can explain such spread patterns of covariability through its "coupled effects on precipitation and wind-driven upwelling" (Peterson & Haug, 2006).

Coral δ^{18}O data from the northwestern Red Sea also registered subtropical Atlantic interannual and interdecadal climate variability related to the North Atlantic Oscillation (NAO) (Felis et al., 2000; Grosfeld et al., 2007). Other paleoclimatic evidences like the Lake Malawi, tropical Eastern Africa, coincide with changes in northern winds blowing over the area, suggesting changes in the intensity of trade winds, related to higher latitude events (Johnson et al., 2002; Baker, 2002).

A recent comparison between Cariaco Basin sediments and coccolithophorid paleorecords in the Norwegian Sea ($\sim 65°$N) also show the close relationship between the two areas (Fig. 1.3). Registers of low sea temperatures in the high latitude region record are coherent with periods of low rainfall in the Cariaco Basin at different timescales, and vice versa (personal communication with Eystein Jansen). On long timescales, this warmer then normal conditions in the northern North Atlantic seem to coincide with the ITCZ extending further to the north than normal.

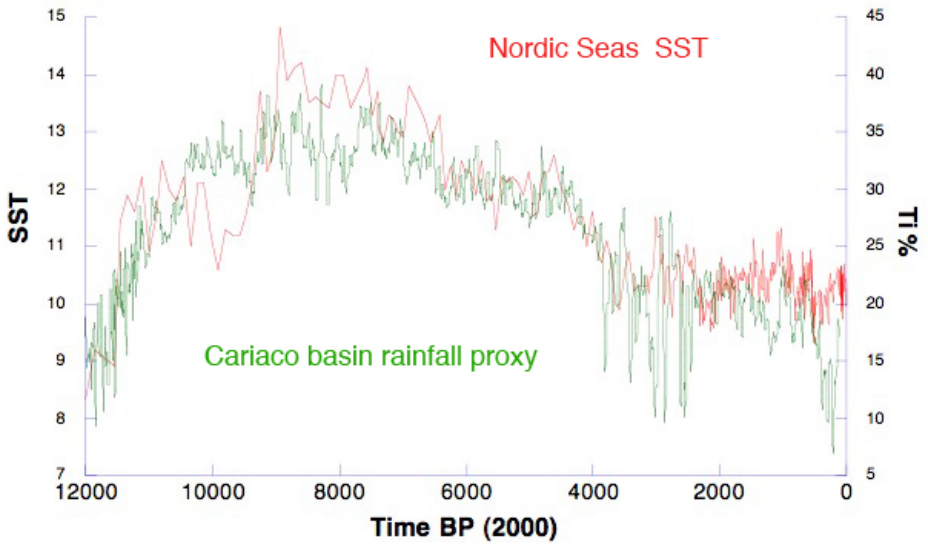

Figure 1.3: Covariability of paleorecords in Cariaco Basin and the Norwegian Sea. %Ti in the sediments is interpreted as a proxy for rainfall and terrigenous input in the Cariaco Basin (Peterson & Haug, 2006), while U_{37}^{K} abundance provide good estimates for Norwegian Sea temperatures (Calvo et al., 2002; Risebrobakken et al., 2003). Low %Ti in the Cariaco Basin proxy roughly match low temperature registers in the Norwegian Sea, at different timescales. Unpublished data; Personal communication with Eystein Jansen, Bjerknes Centre for Climate Research, Bergen, Norway.

Moreover, the suggestion of teleconnections between the Atlantic tropics and northern high latitudes do not rely only in paleoclimatology. Modern off-equatorial atmospheric circulation anomalies seem to force anomalous SST meridional gradients, affecting the position of the ITCZ and consequently precipitation pattern over equatorial Atlantic areas, such as the Nordeste of Brazil (Nobre & Shukla, 1996), the Sahel, Africa (Folland et al., 1986) and the Middle East (Felis et al., 2000).

Despite the continuous findings, modern Atlantic high latitude teleconnections with the tropics are not completely described or understood, specially the unresolved influences in the decadal timescale in tropical Atlantic climate (Nobre & Shukla, 1996).

This study investigate patterns of teleconnections in the North Atlantic, more specifically how the Norwegian Sea SST relates to the Caribbean Sea climate variability, using instrumental data of sea surface temperature (SST) and sea level pressure (SLP) anomalies as the main climatic variables. The working hypothesis is that changes in the northern North Atlantic SST may be linked to the interhemispheric SST and SLP, and associated with the position of the ITCZ. As such relations are indicated by proxy data, similar patterns could perhaps be present as a modern mode of interannual to decadal variation.

The main questions raised in this work are the following:

1. Is the covariability indicated in paleo records for past climate seen today? If so, what is the temporal and spatial characteristic scales of this covariability?

2. What could possibly drive the reported covariability of the position of the ITCZ and the high latitude North Atlantic SST in the paleo records?

3. Can modern atmospheric and oceanic circulation dynamics explain present and past climate teleconnections between the northern North Atlantic and the tropical Atlantic?

To solve these questions, a fundamental problem that needs to be explored is what drives the ITCZ and the North Atlantic variability. The answer to this will help the understanding of the correlations found in the records of the past.

This thesis is organized as follows: In the introductory chapter a short review of teleconnections worldwide and the evidences of relationships between North Atlantic and tropical regions climate has been given. In Chapter 2 a brief description of the background state of atmospheric and ocean circulation variability of the North Atlantic is presented in order to give the reader the necessary background for the further results and discussion. In Chapter 3 the data are presented and the applied statistical approach is discussed. The results are given in Chapter 4 and in Chapter 5 the various results are discussed. Chapter 6 concludes the thesis with a summary and conclusion.

Chapter 2

A short review of the North Atlantic climate variability

2.1 North Atlantic Oscillation (NAO)

The NAO is the only teleconnection pattern evident throughout the year in the North Hemisphere and is the most important persistent pattern identified in the region (Marshall et al., 2001; Hurrell et al., 2006). It has one of its centers of oscillation nearly overlapping the Azores High, while the other center is located southwest of Iceland (close to the Icelandic Low) (Marshall et al., 2001). NAO indices that measure its intensity and phase, are derived either from normalized, time averaged pressure differences in SLP between Lisbon, Portugal minus Stykkisholmur, Iceland, or from the principal component (PC) of the leading empirical orthogonal function (EOF) of boreal winter SLP. During this season, the NAO signal is more intense, since the atmosphere is more active and perturbations reach their maximum amplitudes. As a result, the influence of the NAO on surface temperature and precipitation is greater at this time of year (Hurrell et al., 2006).

The impact of the NAO has been widely recognized (Marshall et al., 2001; Hurrell et al., 2006) (Fig. 2.1). It is directly responsible for the enhancement (or decrease) of the westerlies during positive (negative) phases of NAO, when the SLP anomalies over the Azores area are more positive (negative), while the low pressure in the sub-Arctic region is deeper (shallower), resulting in a stronger (weaker) meridional pressure gradient. Unusually strong westerlies lead to shifts in storm tracks in the North Atlantic, affecting advection of moisture over Europe and northern Africa, modifying rainfall distribution and wintertime temperatures. Drier than normal conditions over northern Africa and south Europe occur during the positive phases, while Iceland and northern Europe experience stormier conditions. Impacts in North America have also been documented, although effects are not so strong as they are in Europe and North Africa. During negative phases of the NAO, less storms reach Scandinavia and Iceland, and south Europe and northern Africa become more rainy.

A tripole structure is the oceanic response to the atmospheric forcing of NAO on monthly and seasonal timescales, with larger amplitudes during the winter when the NAO is more en-

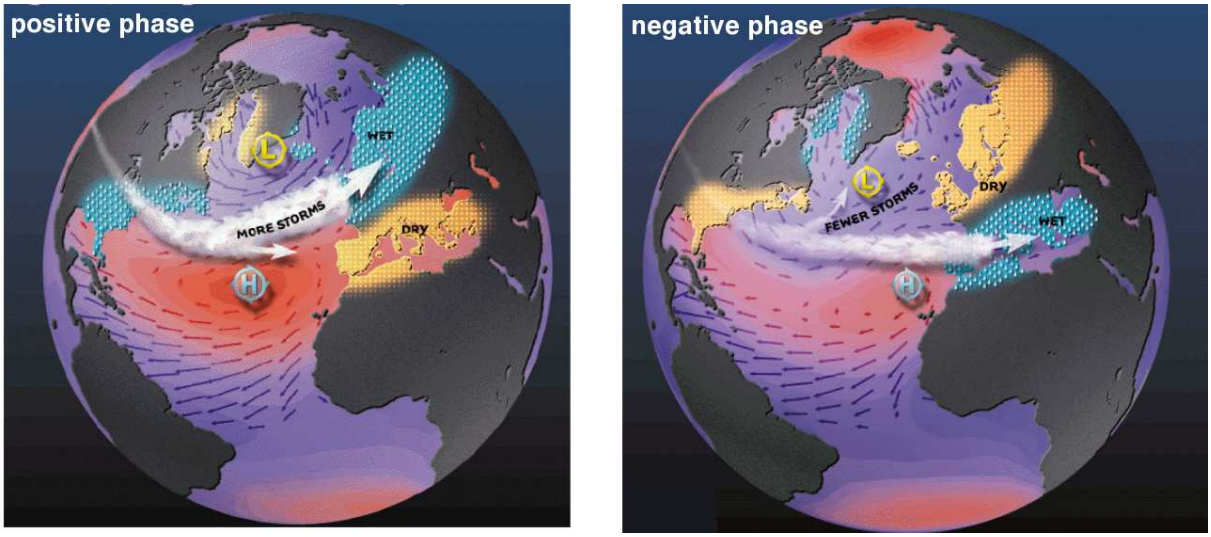

Figure 2.1: North Atlantic Oscillation (NAO) and some of the related impacts over Europe and North Africa. During positive phases of NAO (left), the center over the Azores High is more intense, and most of the storms tracks are deviated northeast, leading to a wetter than normal northern Europe, and drier than normal north Africa and south Europe. Negative phases (right) show a contrary pattern. From http://www.ldeo.columbia.edu/res/pi/NAO/.

ergetic (Marshall et al., 2001; Czaja & Frankignoul, 2002). During a positive NAO phase cold anomalies develop in the subpolar and in the tropical North Atlantic and a warm anomaly occurs at $\sim 40°$N off North America. This relationship arises because stronger winds increase evaporation, resulting in a greater heat loss from the sea surface, followed by a decline in SST (Bjerknes, 1964). It means that SST anomalies are driven by changes and feedback between the air-sea heat fluxes and surface wind related to the phase and the strength of the NAO (Marshall et al., 2001; Czaja & Frankignoul, 2002; Hurrell et al., 2006). Thus, on short timescales, i.e. cycles of less than 10 years, the SST variability in the North Atlantic is driven by the atmosphere and dynamical air-sea feedback. It means that the ocean adjusts itself to the changes in local and non-local surface wind (modified by variations in the SLP), what directly affect the heat-fluxes, changing the SST patterns (Bjerknes, 1964; Kushnir, 1994; Marshall et al., 2001; Hurrell et al., 2006).

It is mostly accepted that the variability of the NAO arises from the internal dynamics of the extratropical atmosphere as a result of interactions between the mean flow and synoptic-timescale eddies. Because the number and intensity of storms varies stochastically from year to year, the spectrum of frequencies of the NAO is much like a white noise process, making NAO's predictability difficult. Still, in the past decades, the NAO has experienced a reversal from predominantly negative to positive phases (Marshall et al., 2001), suggesting a low frequency variability.

Atmospheric models forced with observed global SST were able to reproduced most of the NAO's low frequency variability. For instance, Rodwell et al. (1999) have shown that the tripole pattern of SST is able to create atmospheric patterns similar to the NAO, which primarily

produced the tripole. Over the years this mechanism could contribute to the NAO's "reddening", in a similar way to what has been seen during the last decades. Moreover, Hoerling et al. (2001) have shown that distant forcing from Indian Ocean high SST might also interfere with the NAO on long timescales. As SST variability in the global tropics can largely influence the distribution of rainfall and the location of convective processes, the tropics are expected to influence the extratropical circulation, even though the extent to which tropical SST anomalies influence the NAO more than extratropical North Atlantic SST anomalies do, is unclear (Marshall et al., 2001; Czaja & Frankignoul, 2002; Hurrell et al., 2006).

2.2 Tropical Atlantic Variability (TAV)

Changes in the position of the Atlantic Intertropical Convergence Zone (ITCZ) have major impacts on the rainfall in the adjacent tropical land masses, what is specially noticed in the brazilian semiarid Nordeste region, Caribbean and sub-Saharan Africa (Nobre & Shukla, 1996; Giannini et al., 2000; Xie & Carton, 2004). The seasonal cycle, simply due to the different insolation during summer and winter, is the main factor affecting the variability in the tropics. On longer timescales, such as interannual or interdecadal, equatorial SST zonal gradient, tropical convection, zonal wind and thermocline depth interact in an air-sea coupled mode (Giannini et al., 2000; Xie & Carton, 2004).

Today the seasonal migration of the ITCZ (Fig. 2.2) is regulated by the convergence of the southeast and northeast trade winds, the position of the subtropical highs, the meridional SST gradient around the equator and low surface pressure conditions (Nobre & Shukla, 1996; George & Saunders, 2001; Souza & Cavalcanti, 2009). For instance, the displacement of both Atlantic subtropical highs southward (in the North and the South Atlantic), affects the distribution of the wind field and the position of the trade winds. When tropical North Atlantic SST are colder than the sea surface temperature anomalies in the South Atlantic, changes in the surface pressure associated with SST dipole, intensify and displace the wind confluence southward, and give rise to the conditions favorable to the development of the ITCZ convection south of equator in late winter and early spring, over the warmer SST anomalies of the dipole located southward. A northern position of the ITCZ depends on a relative warming of tropical North Atlantic and cooling of tropical South Atlantic, reversing the equatorial SST gradient, which displaces the ITCZ northward (Hastenrath, 2006). Thus, the cross-equatorial SST gradient (Fig. 2.2) modulate the mean position and strength of the ITCZ, and their interaction is stronger at the end of boreal winter and beginning of spring (March to May) when the equatorial region is "uniformly warm" and the ITCZ is at its southernmost position (Nobre & Shukla, 1996; Ruiz-Barradas et al., 2000; Xie & Carton, 2004; Hurrell et al., 2006).

Remote influence from ENSO and NAO are also involved in the tropical Atlantic variability. The equatorial Pacific affects indirectly the north part of the tropical Atlantic through the Pacific North American (PNA) teleconnection pattern, the zonal "seesaw" in SLP between the tropical Atlantic and the eastern equatorial Pacific (Giannini et al., 2000). Changes in the tropical Pacific convection, associated with ENSO, and anomalies in the Walker circulation

strongly influence the ITCZ (Ruiz-Barradas et al., 2000; Giannini et al., 2000; Chiang et al., 2002; Xie & Carton, 2004; Hastenrath, 2006). For instance, during a warm El Niño phase, when there are warmer SST and lower SLP in the eastern Pacific, higher than normal SLP and lower SST occur in the tropical Atlantic due to a southward displaced North Atlantic subtropical high (Giannini et al., 2000). Additionally, the contribution of each of these mechanisms varies seasonally. The influence of ENSO and NAO is stronger during boreal winter, when their own intensity is higher. Thus both the ENSO and NAO also modify the intensity of the trade winds, affecting the tropical SST gradient of anomalies and the wind-evaporation mechanism, although the local ocean-atmosphere interaction has the dominant role in the tropical sector (Wu & Liu, 2002).

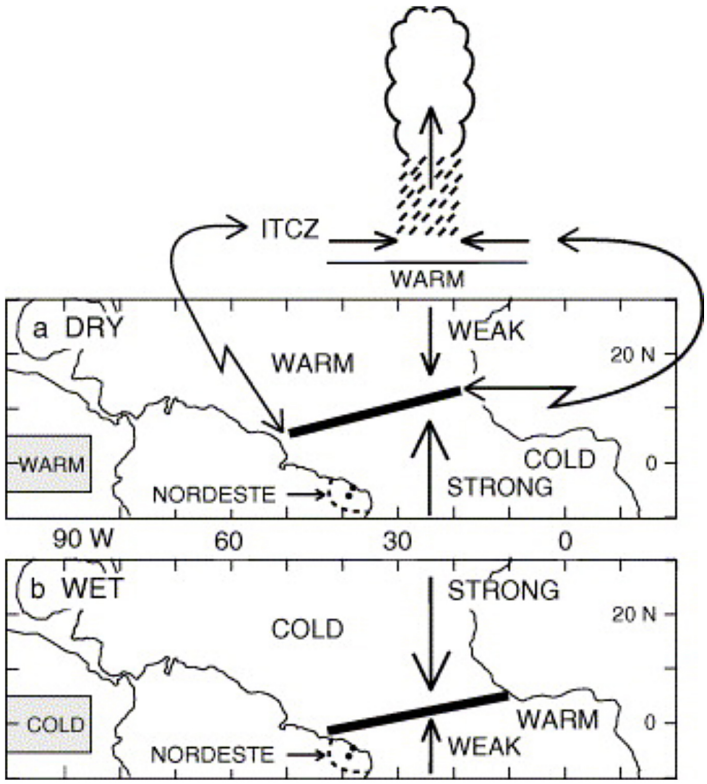

Figure 2.2: Illustration of the SST gradient, northeast and southeast trade winds configuration involved in setting the meridional mode, which affects the position of the ITCZ and the rainfall in the tropical Atlantic. The brazilian Nordeste region is indicated, as well as the simultaneous influence of the tropical Eastern Pacific. From Hastenrath (2006); his Figure 3.

2.3 Meridional overturning circulation (MOC)

The poleward transport of heat, salt and nutrients, is mainly achieved by the meridional overturning circulation (MOC), also denoted as the thermohaline circulation (THC). Air, sea, ice and freshwater interactions allow that warm waters moving poleward, loose heat, increase in density and sink at high latitudes at different subduction zones in the Nordic Seas and the Labrador Sea. The water then flows equatorward as the North Atlantic Deep water (NADW)

(Delworth & Greatbatch, 2000). The main currents (Fig. 1.2) that transports tropical waters to higher latitudes are the Gulf Stream, the North Atlantic current and the Norwegian Atlantic current. When the Gulf Stream reaches $\sim 40°$N it separates from the North American coast and splits into smaller branches. The North Atlantic current then follows northward and enters the Nordic Seas moving between Iceland and Scotland.

Fluctuations in the MOC have been indicated as the possible onset for abrupt and worldwide climate changes registered in paleoclimatic records (Stocker, 2003; Alley et al., 2003; Broecker, 2003). Modelling studies showed that freshening in high latitude seas, due to warming and melting of glaciers and sea-ice, affect the intensity of the MOC (Marshall et al., 2001; Broecker, 2003). Models response to a complete shutdown of the thermohaline circulation, lead to a widespread cooling in the Northern Hemisphere and changes in the cross-equatorial SST gradient and tropical rainfall (Chiang & Koutavas, 2004).

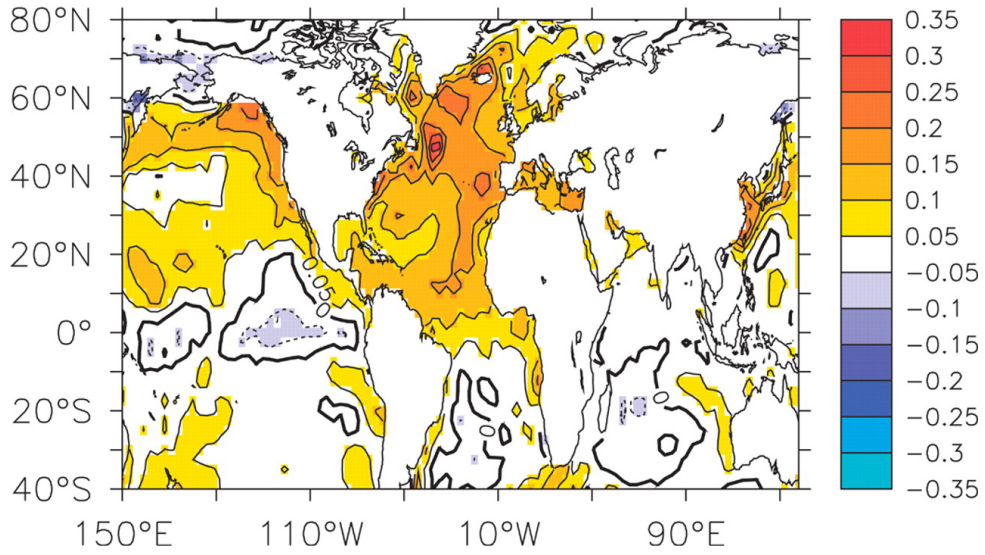

Figure 2.3: The basin wide AMO SST pattern. Anomalies have the same sign in most of the Northern Hemisphere. The pattern was obtained regressing the SST onto the normalized AMO index. From Sutton & Hodson (2005); their Figure 1.

The Atlantic Multidecadal Oscillation, AMO, i.e. variability of the SST patterns in the North Atlantic, is thought to be driven by the MOC (Knight et al., 2005). The spatial AMO pattern of SST variations show anomalies of the same sign over the whole North Atlantic, with larger anomalies east of Newfoundland (Fig. 2.3) (Sutton & Hodson, 2005). This pattern has been related to low frequency variability in the basin and with variations in summertime climate in western Europe and North America (Sutton & Hodson, 2005, 2007). The AMO has also shown significant contribution to the Sahel, brazilian Nordeste and the Caribbean precipitation (Knight et al., 2006). A warm AMO phase is associated with a northward displacement of the tropical rainfall band together with a cross-equatorial wind anomaly, what would thus indicate its influence over the ITCZ, despite that the short instrumental record limits the amount of AMO phases registered (Knight et al., 2006; Sutton & Hodson, 2005).

2.4 Intertropical Convergence Zone (ITCZ)

The Atlantic ITCZ is characterized by a zonal band of low pressure and high precipitation that occurs predominantly over the ocean basin and extends from South America to the west coast of Africa. Convection associated with the seasonal migration of the ITCZ plays a major role in controlling the rainfall over the land masses bordering the tropical Atlantic (Peterson & Haug, 2006). The conditions that define the ITCZ region and give rise to the intense atmospheric convection associated with it, include high SSTs, low surface pressure and the confluence of northern and southern trade winds. This in turn leads to conditions of maximum convergence, and the onset of a well defined band of convective clouds that characterize the ITCZ (Souza & Cavalcanti, 2009).

The effect of the position of the ITCZ over the ocean, and its relation to the intensity of upwelling in tropical areas, specially in the the Caribbean Sea and Cariaco Basin, is described by Peterson & Haug (2006). In the late boreal winter and early spring (January to March), the ITCZ reaches its southernmost position, and strong northeast trade winds in the tropical North Atlantic induce Ekman transport to the northwest in the North Atlantic. These same winds blowing over the Caribbean Sea and the Cariaco Basin result in upwelling during the dry season, when the ITCZ and its associated low pressure and rainfall lie south of the equator (Fig. 2.4). In June and July, the ITCZ moves north to a mean position over the tropics, the trade winds decrease and the upwelling weakens or stop. With the northward migration of the ITCZ the regional rainy season starts and increased fluvial discharge from rivers directly affects Cariaco Basin and the southern Caribbean (Giannini et al., 2000; Peterson & Haug, 2006).

Thus the chain of interactions between these different phenomena can be simplified as follows (Fig. 2.5). The NAO modifies the mean latitudinal position of the westerlies, which are normally centered at 40°N. This north-south displacement of winds in the North Atlantic, interacts with the tropical lobe of the SST anomaly tripole (the positive sign shown in Fig. 2.5 is associated with a negative NAO phase, see Section 2.1). It is closely related to the cross-equatorial SST gradient and trade winds, which in turn has well-known consequences for the ITCZ rainfall over the South and Central America (Nobre & Shukla, 1996; Giannini et al., 2000). Because tropical convection is so important in driving large part of the atmospheric circulation, it is very likely that its position and strength have also some effect over mid latitudes storm tracks. If changes in surface water density occur, induced either by fresher or warmer waters, the strength of the MOC is modified. The NAO is connected with the advection of Arctic cold and freshwater and the air-sea heat fluxes over the North Atlantic, and thus might influence the overturning circulation. Shallow overturning cells can also cause a slow feedback on tropical dynamics. They form as a result of induced Ekman transports in subtropical regions, and can transfer oceanic heat anomalies to tropical upwelling areas, taking part in the interconnections in the basin (Marshall et al., 2001; Hurrell et al., 2006).

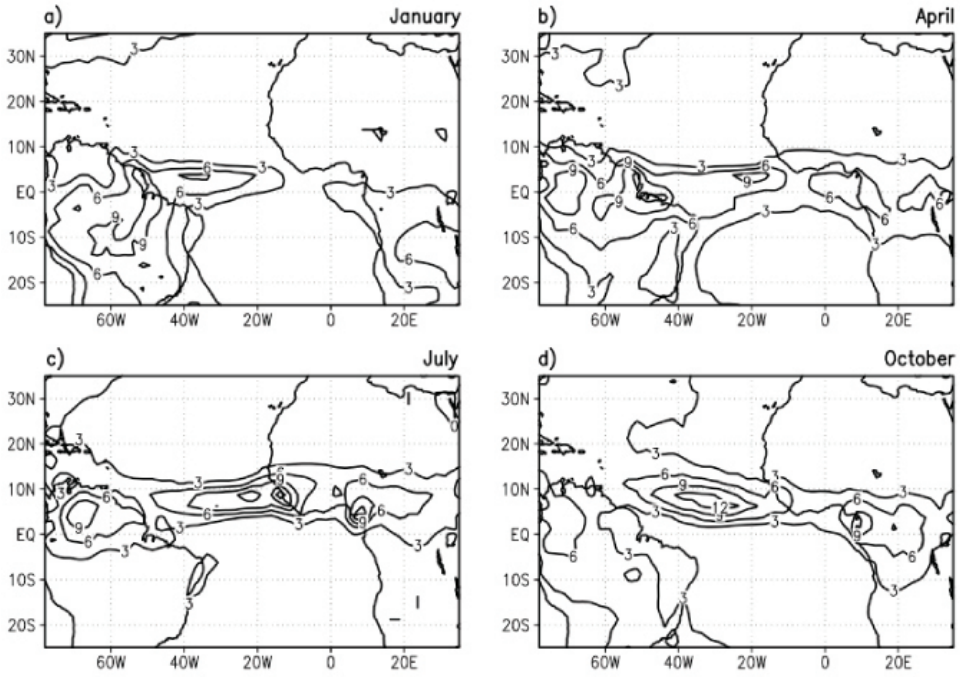

Figure 2.4: Climatological precipitation associated with the ITCZ during representative months of each season. The contour interval is 3 mm/d. From Chiang et al. (2002); their Figure 1.

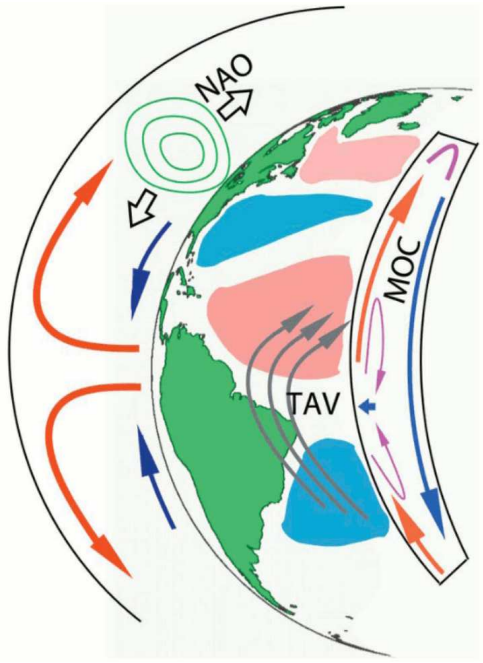

Figure 2.5: Main processes involved in the Atlantic climate variability and their branches of interaction. Green contours indicate the north-south displacement of the mean position of North Atlantic westerlies associated with the NAO. Gray lines illustrate the TAV and the changes in cross-equatorial SST and winds, which are partially controlled by the NAO, its imprint in the sea temperatures and its influence over the intensity of trade winds. As the TAV influences tropical convection, it also may affect the position of the storm tracks in mid latitudes. Both can modify the poleward heat and salt transport, as well as the overturning circulation strength. From Hurrell et al. (2006); their Figure 1.

Chapter 3

Data and Methods

The investigation of teleconnections patterns makes use of straightforward statistics, such as correlations among the variables of interest (Glantz et al., 1991). Another powerful way to look at the structure of the teleconnections themselves is with Empirical Orthogonal Functions (EOFs) which have being widely used in studies of climatological variability (Hannachi et al., 2007). In this work both techniques are applied. Comparison between sea surface temperature anomalies (SST) and sea level pressure anomalies (SLP) are made in order to look for patterns of teleconnections between the Norwegian Sea (NS) in the North Atlantic, and the Caribbean Sea (CS) off the Cariaco Basin in the tropical eastern Atlantic (see Fig. 1.2).

3.1 Data

Updated gridded Kaplan SST anomalies (Kaplan et al., 1998), SLP data from the International Comprehensive Ocean-Atmosphere Data Set project (ICOADS)[1](Woodruff et al., 1987) and Reanalyses SLP data from National Centers for Environmental Prediction (NCEP) and the National Center for Atmospheric Research (NCAR) (Kalnay et al., 1996) are used. Kaplan SST data extend from January 1856 to present, but the ICOADS SLP data has not been updated after July 2001. To include SLP data until August 2008, NCEP/NCAR Reanalyses SLP data, covering from January 1948 to present, and at a resolution of $2.5° \times 2.5°$ was gridded to the same grid as Kaplan's data ($5° \times 5°$), and then merged with Kaplan SLP resulting in a new data set covering 152 years (January 1856 to August 2008). Only missing data from August 2001 to August 2008 have been replaced by the NCEP/NCAR Reanalyses data. The long term annual means of the SST and SLP in the North Atlantic are shown in Figure 3.1. The analysis is limited to the North and tropical Atlantic area (102°W-42°E; 32°S-76°N).

Two boxes are defined in the Cariaco Basin and in the Norwegian Sea to include the position where proxy records of high latitude SST and tropical rainfall were obtained (Haug et al., 2001; Calvo et al., 2002, see Fig. 1.3). The SST and SLP indices are extracted from these areas. The limits for the SLP and SST grids are slightly different and are used to investigate the relationships between these two regions. For the Norwegian Sea they are: 6°W-10°E;60°N-72°N (SLP grid) and 7.5°W-12.5°E; 57.5°N-72.5°N (SST grid). For the Caribbean Sea they are: 74°W-

[1]Since ICOADS data originates from ship observations, land points contain no information.

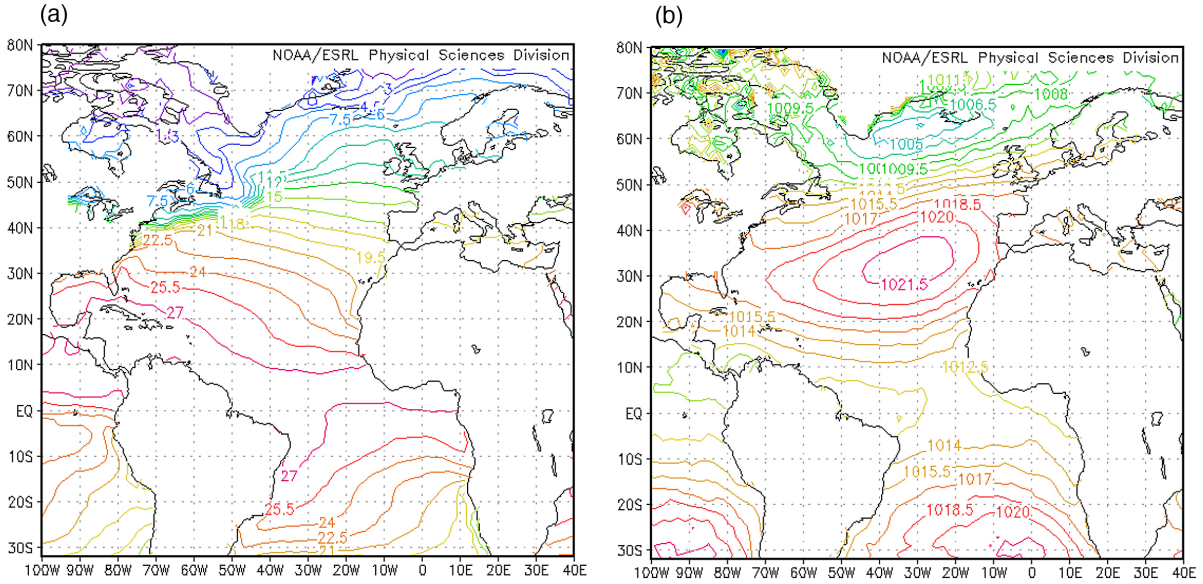

Figure 3.1: Long term annual means of (a) SST (°C) and (b) SLP (mb) in the North Atlantic. Image provided by Physical Sciences Division, Earth System Research Laboratory, NOAA, Boulder, Colorado, from http://www.esrl.noaa.gov/psd/.

62°W; 12°N-20°N (SLP grid) and 77.5°W-62.5°W; 12.5°N-22.5°N (SST grid). The indices are shown in Fig. 3.2.

Prior to the statistical analysis the seasonal means for winter (December, January, February; DJF), summer (June, July, August; JJA) and annual were calculated. This has been done to isolate seasonal components and to obtain a clearer signal of the variability over the years. The areas were then weighted by the cosine of the latitude of each point, to compensate for the unevenly distribution of grid points from the equator towards the pole. Next, the long-term temporal mean and the linear trend from each grid point time series were removed to obtain the anomalies. Note that the series were not normalized in order to keep the variance for the EOF analysis. To investigate the variability on decadal timescales, a running mean filter of 10 years was applied to the time series (Fig. 3.2).

3.2 Correlation Analysis

Correlation and covariance are among the most basic and classical method of time series analysis. As they are used to describe the covariability of two time series as a function of time they are useful tools to look for teleconnections. Even though high correlation between two parameters does not imply a direct "cause and effect", they either represent a close relationship between the two variables or their simultaneous dependence on a third variable (Mauritzen et al., 2006). Lagged covariability is used to investigate delayed responses between the SST and SLP series. Problems may occur for long time lagged correlations, because of the constraint that few samples of low frequency oscillations reduce its statistical confidence (Emery & Thomson, 2001). All the cross-correlations considered the Norwegian Sea SST, the NAO or the AMO index as

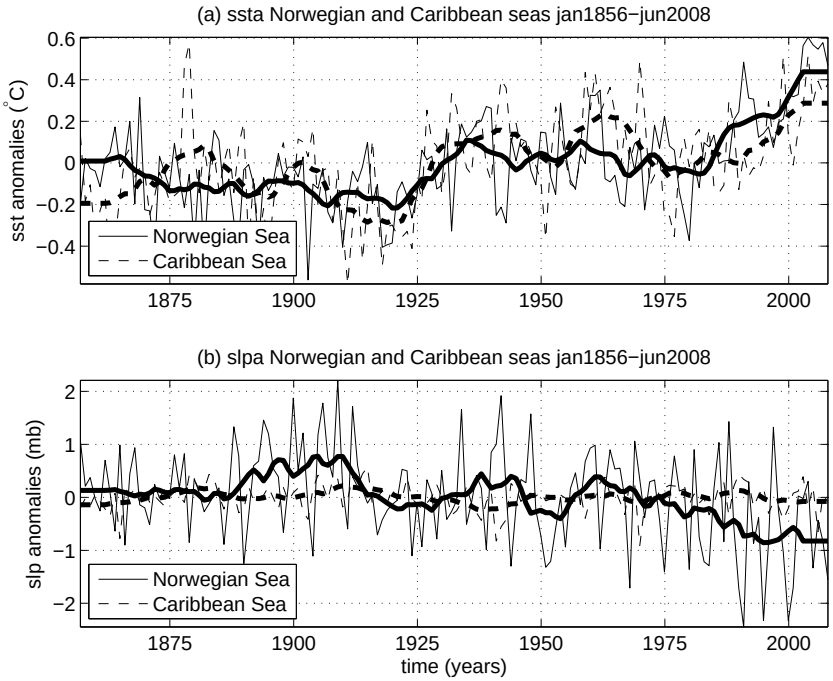

Figure 3.2: Upper panel: Time series of (a) annual and (b) summer means of SST anomalies in the Norwegian and Caribbean Seas obtained from the area averages shown in Fig. 1.2. Bold lines represent the 10 years running mean of the series.

the first argument, so a positive lag indicates that these indices lead the changes of the second variable.

In this study correlation and cross-correlation analysis are performed with the Norwegian SST and Caribbean SST and SLP indices, both for the raw data and for the 10 points running mean filtered data. Correlation maps between the Norwegian Sea SST and the SST and SLP elsewhere in the North Atlantic are also analyzed. The conclusions drawn from the simple linear correlations are based on significant coefficients between the data. To account for autocorrelation in the data sets the real degrees of freedom (df) of the time series (i.e. independent observations) were estimated with the formula found in Mauritzen et al. (2006) and based on Quenouille (1952):

$$N_c = N/(1 + 2r_a^1 r_b^1 + 2r_a^2 r_b^2) \tag{3.1}$$

Here, N_c is the effective number of degrees of freedom, N is the total number of data points (i.e. 152 years, for the 10 points running mean series), r_a^1 and r_b^1 are the lag-one autocorrelation coefficients, and r_a^2 and r_b^2 the lag-two autocorrelation. The significance levels for the correlations are tested with a two tailed t-test, and all the significance levels are set to 99%, unless stated differently (Emery & Thomson, 2001).

In order to understand the relations presented in the correlation maps, two of the most significative indices of climate variability in the North Atlantic, the NAO and the AMO, and their relations to the SLP and SST indices are investigated. Simple linear correlations and

cross-correlation analysis are performed. The EOF procedure described in the next section is an appropriate approach to obtain the associated time fluctuations of the NAO. For the AMO, a 10 years filtered annual mean index[2] is used, since there are only small differences between the annual and seasonal mean indices (Sutton & Hodson, 2005). Following previous studies where regressions are used to illustrate NAO and AMO's influence on the North Atlantic variability at decadal timescales (Rodwell et al., 1999; Hoerling et al., 2001; Sutton & Hodson, 2005, 2007), both SST and SLP unfiltered fields are also regressed onto the NAO and AMO indices.

3.3 Empirical Orthogonal Functions analysis (EOF)

The EOF is a technique used to decompose spatiotemporal data sets into their leading patterns of variability, which explain most of the variance of the data sets. It is based on the decomposition of the covariance matrix into empirical orthogonal modes, both in the form of a time series (principal components, PC) and the spatial pattern associated to a particular mode of variance (EOF) (Emery & Thomson, 2001). Since the EOF are constructed to explain maximum variance in the first modes, it is expected that the "center of actions of the leading EOF will coincide with the regions of strongest stationary variability" (Hurrell et al., 2006). The first mode contributes with the highest variance of the data, while the second explains the variance that is not explained by the first mode. The different modes are also orthogonal in space and time, therefore they are uncorrelated. Because of the constraint of orthogonality between the spatial (EOF) and temporal (PC) modes, EOF should be interpreted carefully. Additionally, the EOFs can be quite sensitive to the spatial domain or the time period designated for the analysis. For this reason the areas for EOF analysis are slightly distinct from the areas of the correlation maps. This artifact is used to assure that the variance explained by each mode is comparable to previous studies.

The Singular Value Decomposition (SVD) is one of the methods available to calculate EOF, and is based in the decomposition of a matrix D $m \times n$ into the form:

$$D = USV^T \tag{3.2}$$

where U is $m \times n$ column-orthogonal, S is a $n \times n$ diagonal matrix and V_T is a $n \times n$ orthogonal matrix (Emery & Thomson, 2001).

In this study, the matrix D was the spatiotemporal data of SLP and SST with the space in first dimension (m rows) and time in the second (n columns). The contrary could also be used if there were more temporal points than spatial ones, because the only differences between U and V is how the singular values of S are grouped, and which variable holds the spatial function and which with the temporal function (Emery & Thomson, 2001). Here, the matrix U gives the spatial pattern, the matrix S gives the amplitudes, i.e. variance, explained by each mode and the V provides the time history associated with the spatial pattern. The EOF analysis was computed with the built-in $MATLAB^{®}$ *svd*-function.

[2]From http://www.cdc.noaa.gov/data/correlation/amon.us.long.data.

Chapter 4

Results

4.1 Time series

In Figures 4.1 and 4.2 the annual and summer filtered time series of SST and SLP anomalies in the Norwegian and the Caribbean Seas are shown. The filtered series of SST, showing the interdecadal variability, are positively correlated, with highest correlation coefficients (r) found in summer ($r = 0.75$). A negative phase is found when correlating annual NS-SST with CS-SLP ($r = -0.42$, significant at the 95% level of significance). There are no significant correlations between filtered NS-SST and CS-SLP during winters. If years with the positive trend in the SST series after 1975 are removed, correlations between the filtered NS-SST and the CS-SLP for annual, summer and winter means increase to -0.66, -0.65 and -0.49, respectively. Although this final trend likely interferes the analysis of the correlation maps, all the period (1856-2008) is still used, since it can be considered that the NS-SST and the CS-SLP have a valid and coherent covariability.

The correlation coefficients found for unfiltered data, representing the interannual variability, are low, but significant, specially for the relations between the Norwegian Sea SST and Caribbean Sea SLP. The correlation between the Norwegian Sea SST and the Caribbean SST, for annual means equals 0.32, while the winter correlation coefficient between the NS-SST and the CS-SLP equals 0.26. In Table 4.1 the correlation coefficients between the SST and SLP time series for the two areas given in Fig. 1.2 are shown.

Cross-correlation between unfiltered data is not shown because of the few and low significant coefficients found at other lags, but cross-correlation between the filtered SST indices are high at zero time lag and also show a negative peak at approximately 80-85 years (Fig. 4.3). Short instrumental record limits the interpretation at this timescales. The cross-correlation of the filtered NS-SST and CS-SLP is weaker, but significant at approximately 3 years lag during summer, and at no time lag for the annual means (both significant at the 95% level).

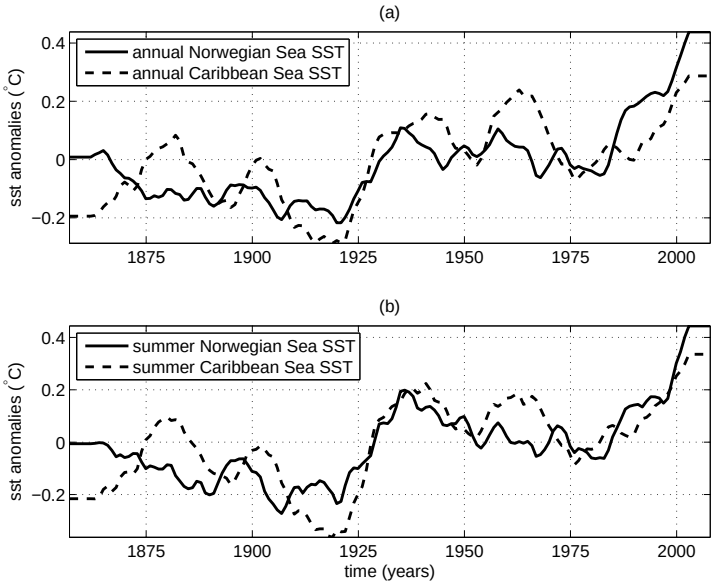

Figure 4.1: Covariability between the 10 years running mean Norwegian and Caribbean Seas SST indices in instrumental record. (a) Upper panel shows the annual means of the SST indices (r=0.70) and (b) lower panel, the summer means (r=0.75). All r are significant at the 99% level.

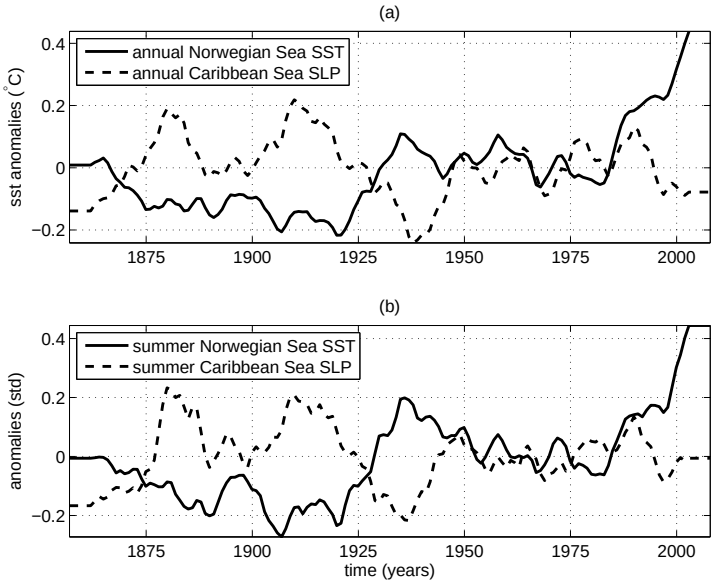

Figure 4.2: Covariability between the 10 years running mean Norwegian Sea SST and Caribbean Sea SLP indices in instrumental record. (a) Upper panel shows the annual means of the indices (r=-0.42) and (b) lower panel, the summer means (r=-0.38, both significant at the 95% level).

Table 4.1: Correlation coefficients (r) between the SLP and SST indices from the Caribbean Sea and the Norwegian Sea SST index. Raw data and 10 years running mean filtered data are indicated. Highest coefficient values are in bold. One (*) or two (**) asterisks indicate that the correlations are significant at the level of significance at 95% or 99%, respectively. Significance level is adjusted for autocovariance reducing the effective degrees of freedom *df*.

	Caribbean Sea			
	SST		**SLP**	
	raw data	10 yrm	raw data	10 yrm
Norwegian Sea SST (r)				
annual	$\mathbf{0.32^{**}_{df70}}$	0.70^{**}_{df30}	–	$\mathbf{-0.42^{*}_{df30}}$
winter	0.30^{**}_{df90}	0.64^{**}_{df30}	$\mathbf{0.26^{**}_{df100}}$	–
summer	0.28^{**}_{df100}	$\mathbf{0.75^{**}_{df30}}$	–	-0.38^{*}_{df30}

4.2 Empirical Orthogonal Functions

The leading EOF calculated from monthly SLP anomalies in the North Atlantic (Fig. 4.4) is characterized by a surface dipole, the well known pattern of the North Atlantic Oscillation (NAO) described in many other studies (Marshall et al., 2001; Furevik & Nilsen, 2005; Hurrell et al., 2006). The NAO pattern in the North Atlantic area accounts for approximately one third (or more) of the total variance of the SLP field. The second mode, also known as the East Atlantic Pattern (EAP), exhibits a monopole pattern over the northeast area of the North Atlantic. It explains 27% of the atmospheric variability in the region.

The NAO index was obtained from the first principal component of the leading EOF of SLP of DJF (boreal winter). It represents the temporal oscillations of the NAO pattern, (Fig. 4.6a), and it correlates very well (r=0.86) with the station based index for DJF (Hurrell, 1995)[1].

The EOF modes of the SST over the North Atlantic are shown in Fig. 4.5. The first mode of SST variability in the North Atlantic consists of a tripolar feature, which during a positive NAO phase is associated with a cold anomaly in the subpolar North Atlantic, a warm anomaly in the middle latitudes centered off North America coast (around 40°N), and a cold subtropical anomaly between the equator and 30°N. Here this structure is well defined and explains up to 20% of the variability of the North Atlantic SST. This pattern has also been found in earlier studies (Marshall et al., 2001; Hurrell et al., 2006). The second mode explains approximately 16% of the variance in this area.

[1]From http://www.cgd.ucar.edu/cas/jhurrel/indices.data.html#naostatseas.

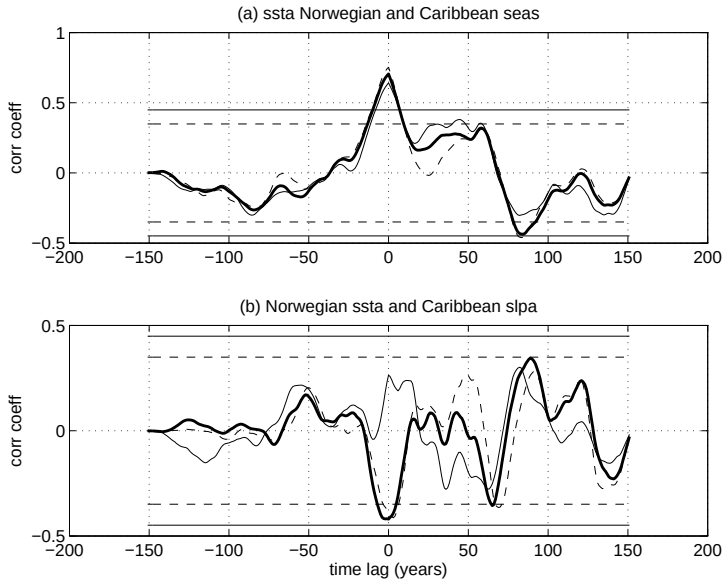

Figure 4.3: Cross-correlation between (a) Norwegian and Caribbean Sea SST and (b) Norwegian Sea SST and Caribbean Sea SLP. Different weighted lines represent the annual (bold line), winter (continuous) and summer (dashed) means. Dashed horizontal line indicates the 95% significance level, while the continuous line indicate the 99% significance level.

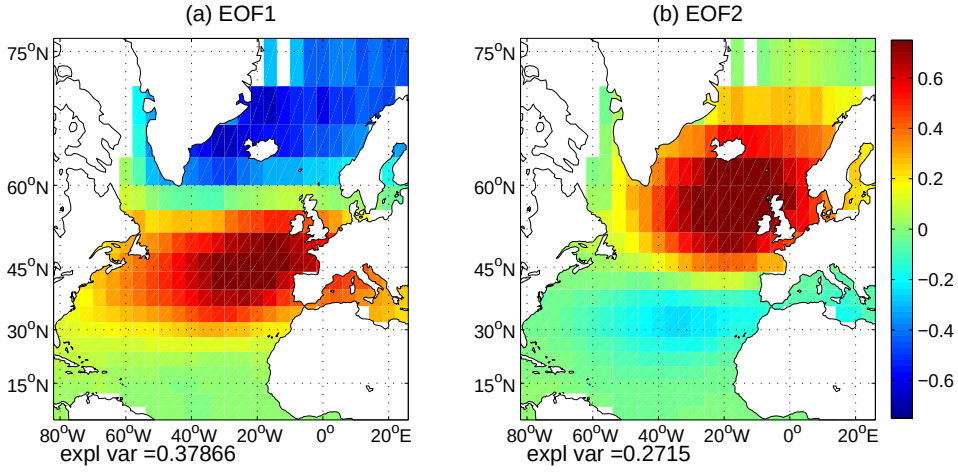

Figure 4.4: First two modes of the EOF for DJF SLP anomalies in the North Atlantic. (a) The first mode resembles the NAO dipole pattern, explaining up to 40% of the SLP variability in the area. (b) The second mode explains 27% of the SLP variance.

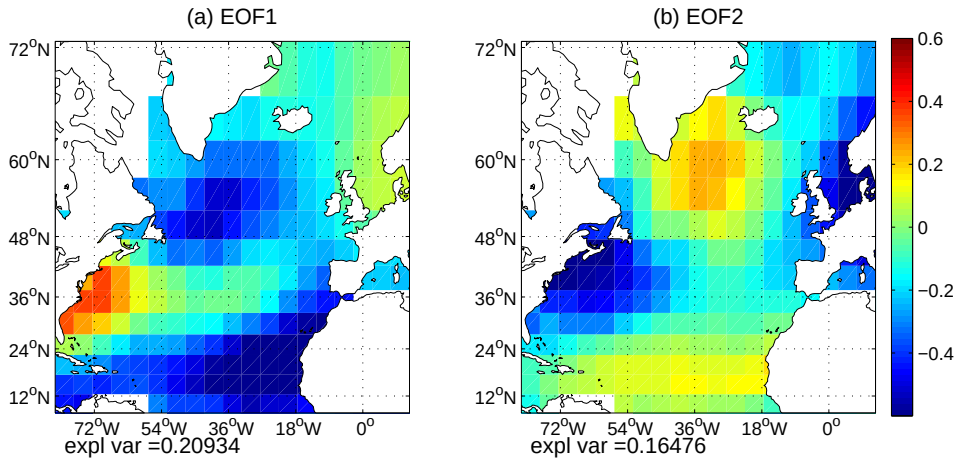

Figure 4.5: First two modes of the EOF for DJF SST anomalies in the North Atlantic. (a) The first mode shows the tripole pattern, associated with the variability of NAO. It explains approximately 20% of the total SST variance. (b) The second mode explains 16% of the variance.

4.3 Linear and cross-correlation analysis

The cross-correlation between each of the raw indices from Norwegian Sea and Caribbean Sea with the first principal component (PC1) of the EOF of DJF SLP field presented in the previous section is shown in Figure 4.7. The PC1 correlates well with the Norwegian (-0.62) and Caribbean (0.46) SLP during the winter, at no time lag. The correlations between the NAO index and the NS-SST ($r = 0.33$) and the CS-SST ($r = -0.20$) are low at lag zero, but still significant at the 95% level.

Because the NAO can be considered as a stochastic variation in the SLP fields of North Atlantic, it is expected that if one filter the highest frequencies that contributes to its "white spectrum" (for instance when using the 10 years running mean filter), most of its physical meaning and impact would be lost (Fig. 4.8). Still, the correlations between the PC1 and the winter CS-SLP (0.62) and NS-SLP (-0.55) are high compared to the r between the NAO index and the NS-SST (0.33). The NAO has no significative correlation with the CS-SST at decadal timescales. Lagged correlations occur at around 50 year time lag for summer CS-SST ($r = 0.48$, at 49 years lag), and the winter CS-SLP ($r = -0.62$, at 55 years lag). Correlation with summer NS-SST is also high at 55 years (0.48), and at -38 yr lag (-0.43). For NS-SLP there is a high correlation for winter and annual means at -35 years lag (0.56). If these relations have physical relevance is hard to determine, because of the relatively short length of time series for low frequency oscillations, and the lack of observational data for ocean circulation.

The cross-correlation analysis between the AMO index and the Norwegian and Caribbean Seas indices is shown in Fig. 4.9 and Fig. 4.10. More organized correlations than with the NAO index are found, specially for 10 years averaged correlations. At interannual timescales the AMO index shows low correlation with the winter NS-SLP ($r = -0.11$) and with the annual CS-SLP ($r = -0.20$). The AMO is slightly better correlated with the annual NS-SST ($r = 0.29$),

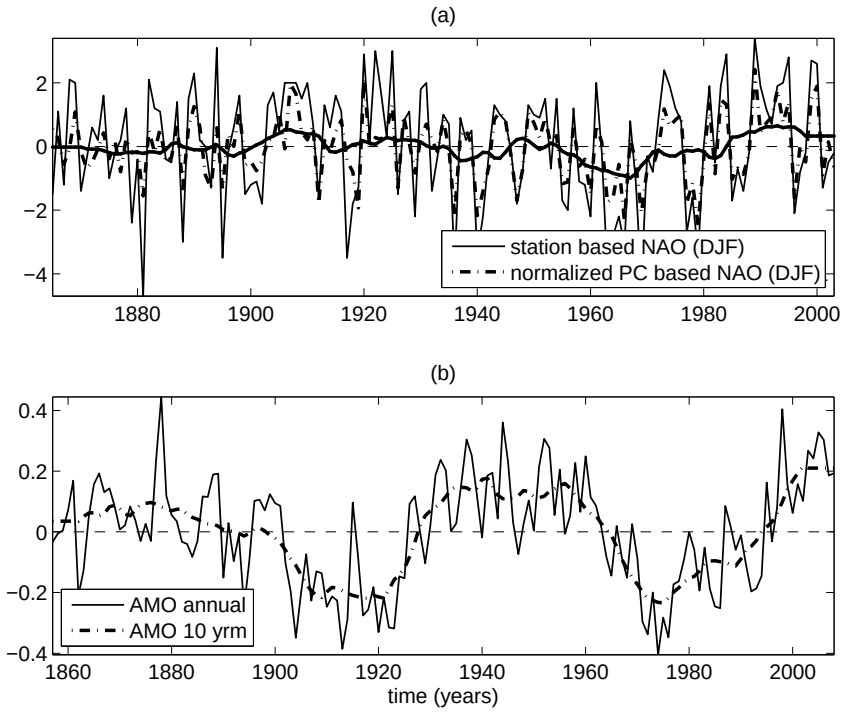

Figure 4.6: (a) The NAO index. Comparison between the NAO station based index (Hurrell, 1995) and the first principal component (PC1) from EOF analysis of DJF SLP field (r=0.86). Thicker line show the smoothed index, in 10 years averages. (b) The Atlantic Multidecadal Oscillation index (AMO). Continuous line is the annual index, while the dashed line is the 10 years running mean filtered index.

Table 4.2: Correlations (r) between the SLP and SST indices from the Caribbean Sea and Norwegian Sea (only SST), NAO and AMO. Raw data and 10 years running mean filtered data are indicated. Highest coefficient values are in bold. One (*) or two (**) asterisks indicate that the correlations are significant at the level of significance at 95% or 99%, respectively. Significance level is adjusted for autocovariance reducing the effective degrees of freedom *df*.

	Caribbean Sea				**Norwegian Sea**	
	SST		**SLP**		**SST**	
	raw data	10 yrm	raw data	10 yrm	raw data	10 yrm
NAO (r)						
annual	–	–	–	–	–	–
winter	$\mathbf{-0.20^{*}_{df125}}$	–	$\mathbf{0.46^{**}_{df125}}$	$\mathbf{0.62^{**}_{df35}}$	$\mathbf{0.33^{**}_{df125}}$	$\mathbf{0.33^{*}_{df35}}$
summer	–	–	–	–	–	–
AMO (r)						
annual	0.44^{**}_{df70}	0.60^{**}_{df30}	$\mathbf{-0.20^{*}_{df100}}$	$\mathbf{-0.55^{**}_{df30}}$	$\mathbf{0.29^{*}_{df60}}$	0.54^{**}_{df30}
winter	$\mathbf{0.47^{**}_{df80}}$	0.46^{**}_{df30}	–	–	0.27^{*}_{df70}	0.46^{**}_{df30}
summer	0.45^{**}_{df80}	$\mathbf{0.64^{**}_{df30}}$	–	-0.43^{*}_{df30}	0.27^{**}_{df90}	$\mathbf{0.60^{**}_{df30}}$

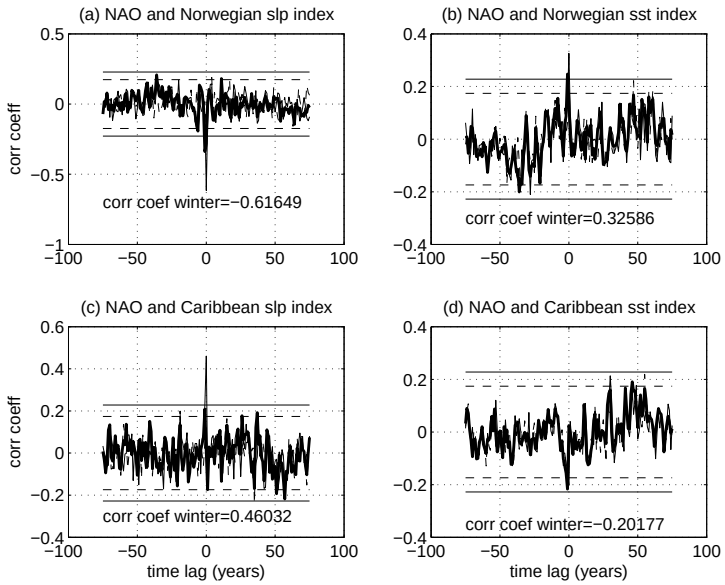

Figure 4.7: Cross-correlation between the PC1 of DJF SLP with Norwegian and Caribbean Seas SST and SLP indices at interannual scales. (a) PC1 and the Norwegian SLP; (b) PC1 and Norwegian Sea SST; (c) PC1 and Caribbean SLP and (d) PC1 and CS-SST. Different weighted lines represent annual (bold line), winter (continuous) and summer (dashed) means. Dashed horizontal line indicates the 95% significance level, while the continuous line indicate the 99% significance level.

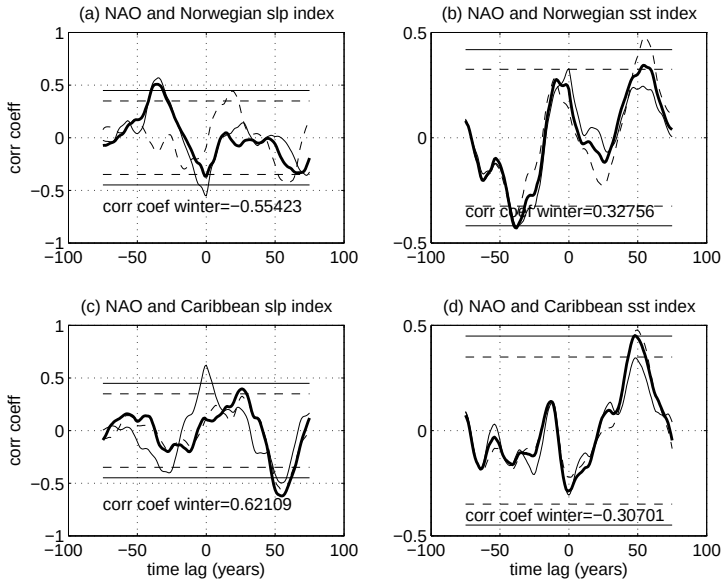

Figure 4.8: Cross-correlation between the 10 year average filtered PC1 of DJF SLP with Norwegian and Caribbean Seas SST and SLP indices. (a) PC1 and Norwegian SLP; (b) PC1 and Norwegian Sea SST; (c) PC1 and Caribbean SLP and (d) PC1 and the Caribbean Sea SST. Different weighted lines represent annual (bold line), winter (continuous) and summer (dashed) means. Dashed horizontal line indicates the 95% significance level, while the continuous line indicate the 99% significance level.

and with the winter CS-SST ($r = 0.47$). The interdecadal correlations show higher coefficients. The r between the AMO and summer NS-SLP index increases to -0.47, and with the annual CS-SLP it raises to -0.55. The correlation between the AMO with Norwegian Sea SST equals 0.60, while with Caribbean Sea SST equals 0.64. A summary of the correlation coefficients r between the NAO, the AMO and the Norwegian and Caribbean Seas indices is given in Table 4.2.

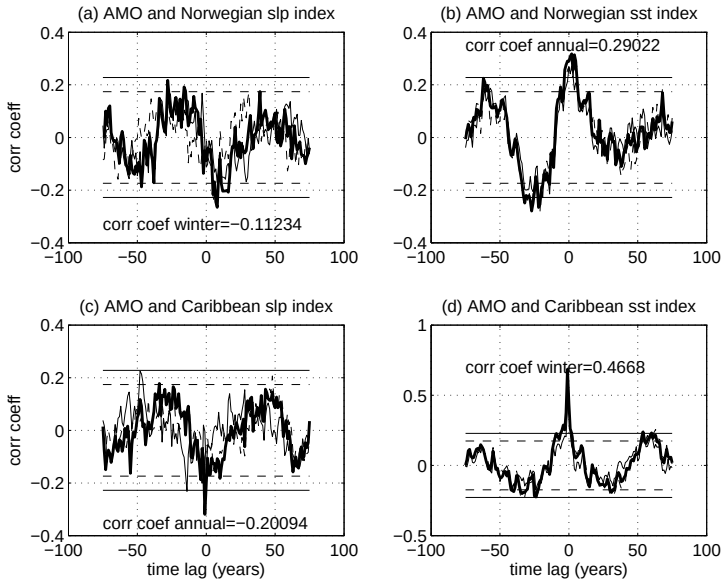

Figure 4.9: Cross-correlation between the AMO with Norwegian and Caribbean Seas SST and SLP indices at interannual scales. (a) AMO index and Norwegian SLP; (b) AMO index and Norwegian Sea SST; (c) AMO index and Caribbean SLP and (d) AMO index and the Caribbean Sea SST. Different weighted lines represent annual (bold line), winter (continuous) and summer (dashed) means. Dashed horizontal line indicates the 95% significance level, while the continuous line indicate the 99% significance level.

The regression map of the unfiltered SST field onto the normalized NAO index (Fig. 4.11) show (a) the SST tripole resulting from (b) the atmospheric NAO forcing at interannual scales. The overall pattern of these maps is the same as the ones obtained with the EOF analysis, and fully described in Section 2.1. The spatial pattern of the SST field regressed onto the AMO index (Fig. 4.11c) is very similar to the monopole pattern of same sign anomalies over the whole North Atlantic describe in the literature (Sutton & Hodson, 2005), and the SLP field regressed onto the same index (Fig. 4.11d) resembles the atmospheric NAO pattern, but with less intense centers of action displaced southwest and with opposite signs from the ones of (b). This same pattern was found by Grosfeld et al. (2007).

4.4 Correlation maps

4.4.1 Norwegian Sea SST and SST anomaly field

Interannual correlation maps between the annual, winter and summer SST data are similar, as shown in Fig. 4.12 a-c. The interannual SST variability shown in these maps exhibits coherent

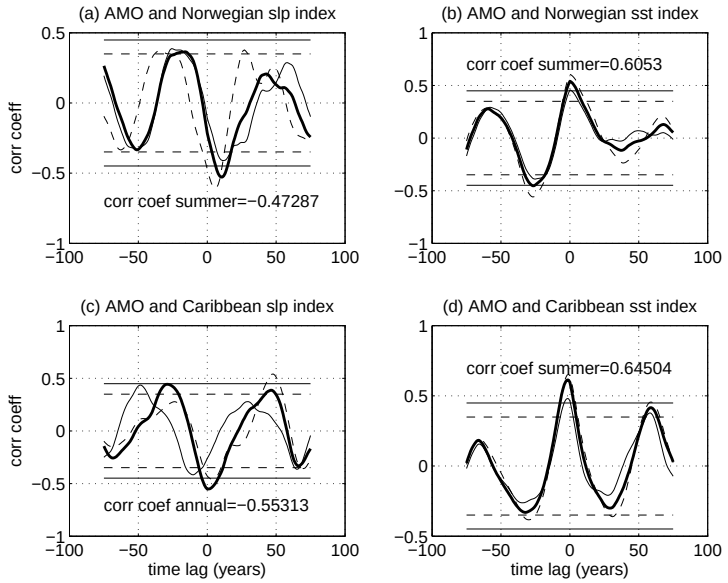

Figure 4.10: Cross-correlation between the 10 year average filtered AMO with Norwegian and Caribbean Seas SST and SLP indices. (a) AMO index and Norwegian SLP; (b) AMO index and Norwegian Sea SST; (c) AMO index and Caribbean SLP and (d) AMO index and the Caribbean Sea SST.Different weighted lines represent annual (bold line), winter (continuous) and summer (dashed) means. Dashed horizontal line indicates the 95% significance level, while the continuous line indicate the 99% significance level.

positive signs between the Norwegian Sea and the subtropical Atlantic, and negative sign with a smaller area southeast of Greenland. During summer, the significant positive correlated area off the west coast of North America centered at $\sim 30°$N has become smaller, and nearly coincides with the positive central area of positive anomalies of the NAO imprint on the SST (Fig. 4.5).

At interdecadal scales ($>$ 10 years) (Fig. 4.12 d-f), the entire North Atlantic is positively correlated with the NS-SST, except for an area southeast of Greenland. The annual, winter and summer means have very much the same patterns, except for minor differences in the winter map, when the uncorrelated areas south of Greenland and approximately at 10°N east of Cariaco Basin is larger compared to the annual and summer means.

4.4.2 Norwegian Sea SST and SLP anomaly field

When examinating the correlation maps for the annual NS-SST and SLP field (Fig.4.13a) a large negatively correlated area occurs over the Nordic Seas and another small positive significant region appears south of Newfoundland. The centers identified in the annual correlation maps are stronger during the wintertime (Fig. 4.13b), where the negatively correlated high latitude area extends over the entire region north of 60°N and the positive center off North America western coast expands southeast. Another positively correlated area appears in the east Atlantic. The interannual summer mean correlation between the SLP field and the NS-SST show no significant correlations (Fig. 4.13c), except for a small negatively correlated region off the Peruvian coast, in the eastern tropical Pacific.

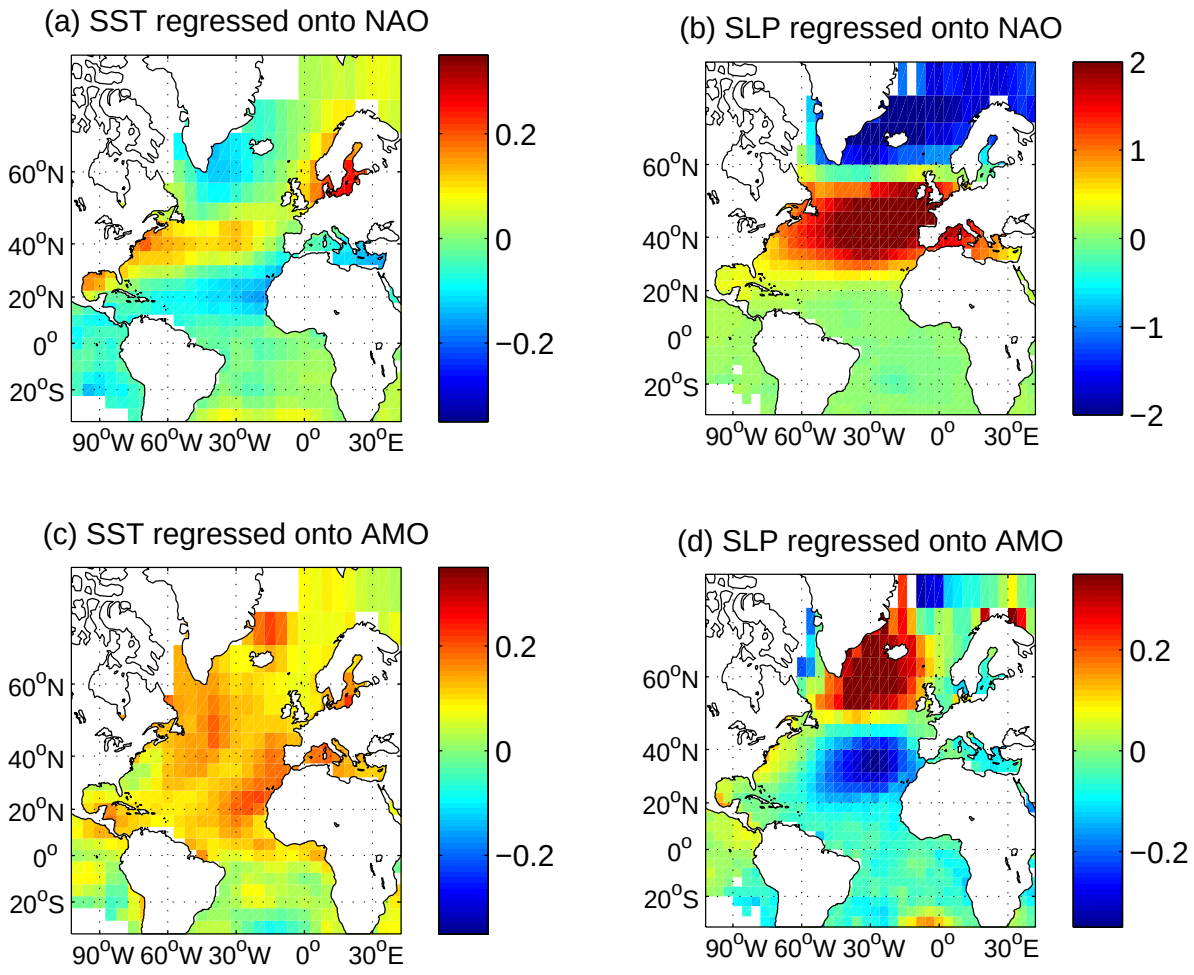

Figure 4.11: Maps of (a) the winter SST and (b) winter SLP fields regressed onto the NAO index, (c) annual SST and (d) annual SLP fields regressed onto the AMO index. AMO index is 10 years averaged (dashed line in Fig. 4.6b), but NAO index and the SST and SLP fields are not filtered. Both indices are normalized (unit variance). Note the different scale in the color bar in (b).

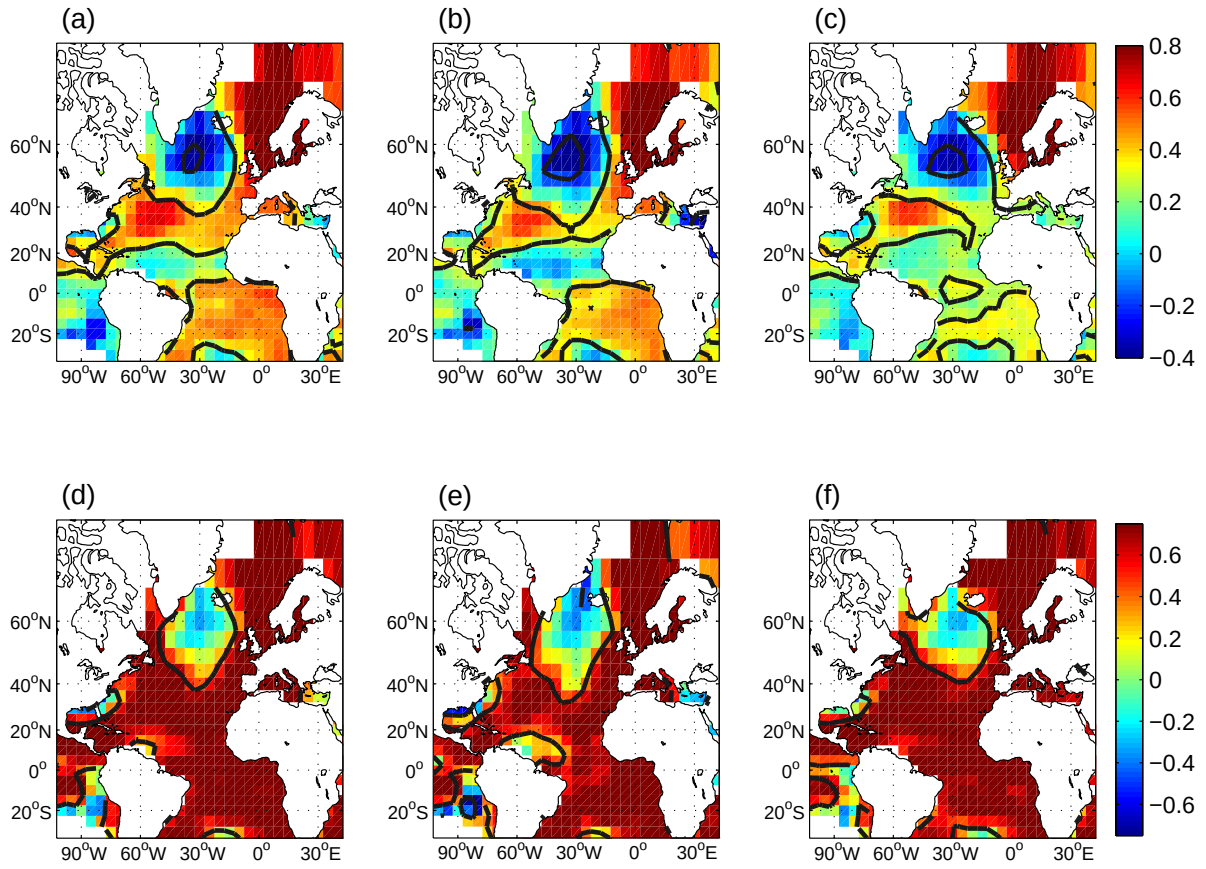

Figure 4.12: Norwegian Sea SST index correlated with SST field elsewhere. (a,d) show the annual means, (b,e) the winter means and (c,f) the summer means. Upper panels display the raw correlations and lower panels the 10 years running average. Areas within the black contour lines (outside the contour for the lower panels) exceed the 99% confidence level of a 2-tailed t-test.

When correlating the NS-SST with the 10 years filtered SLP anomaly field, three centers are identified: one negative over the Nordic Seas, another positive close to Newfoundland and a significant negative correlated area just north of the Cariaco Basin in the annual and summer maps. At summer, another negatively correlated area appears at $\sim 30°$N in the east Atlantic, and is more intense than the signal in the Nordic Seas. From the raw and filtered correlation maps it is clear that the centers identified are related, indicating that the mid and high latitude correlated areas are persistent features both at the interannual and decadal timescales.

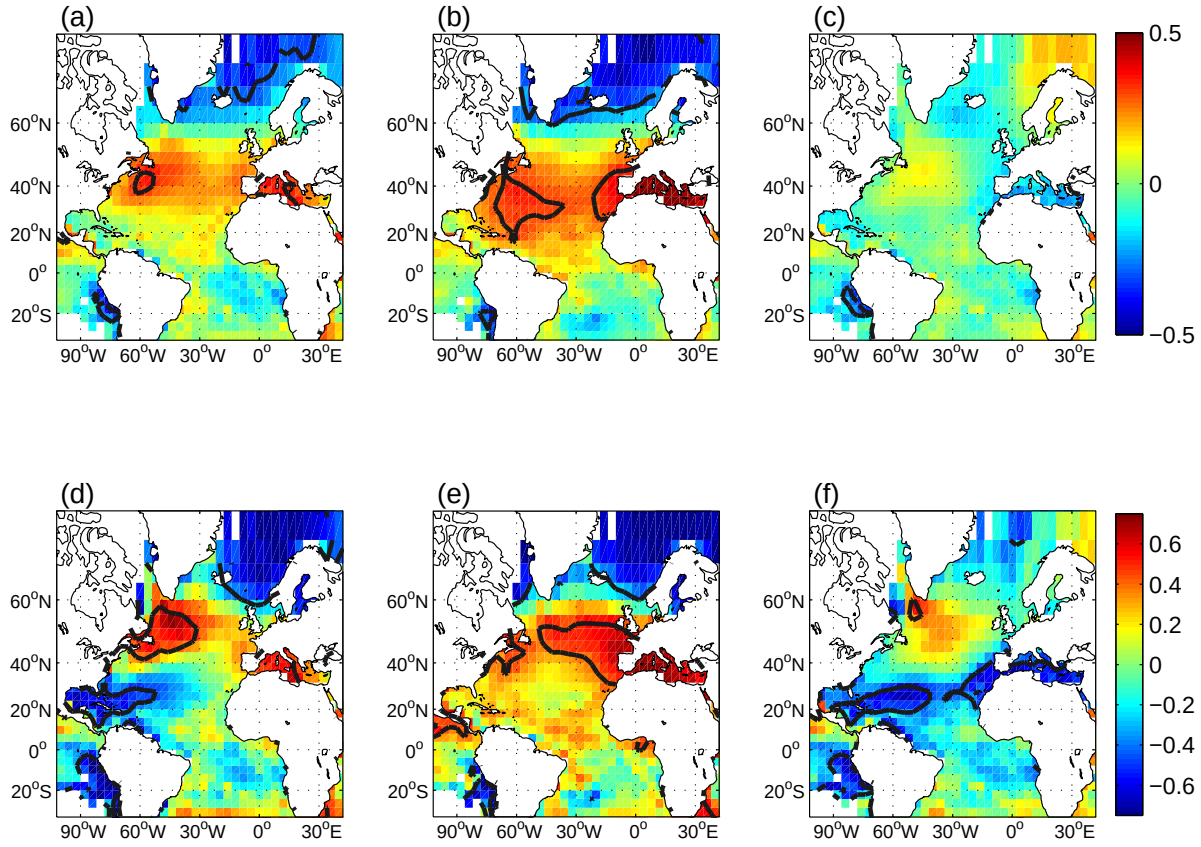

Figure 4.13: Norwegian Sea SST index correlated with SLP field elsewhere. (a,d) show the annual means, (b,e) the winter means and (c,f) the summer means. Upper panels display the raw correlations and lower panels the 10 years running average. Areas within the black contour lines exceed the 99% confidence level of a 2-tailed t-test.

Chapter 5

Discussion

In this study, interannual correlations between the Norwegian and Caribbean Sea instrumental SST and SLP indices are found to be weak, while interdecadal correlations show stronger relations. Correlation between the Norwegian SST and SLP strengthens if only years prior to 1975 are considered. The shift in the temperatures after mid 1970 has been described elsewhere (Furevik & Nilsen, 2005; King & Kucharski, 2006; Grosfeld et al., 2007) and occurs at the same time as the global warming accelerates during the last decades. The results also indicate that decadal scale SST and SLP variability registered in the tropics shows a connection with the SST in high latitudes, as previously indicated by trade wind variability and rainfall proxy records (Black et al., 1999; Peterson & Haug, 2006, respectively).

One of the possible mechanisms to explain these relationships is the NAO. The NAO is highly correlated with the Caribbean and Norwegian Sea SLP, both at interannual and decadal timescales. This is only true during wintertime, in agreement to the fact that its year to year atmospheric impact is stronger during this season, with its intensity weakening in the following months (Marshall et al., 2001; Hurrell et al., 2006). The NAO is known to have strong impacts on the variability of the westerlies and the eastern trade wind system in the North Atlantic, controlling the wind speed variability (George & Saunders, 2001) and the position of the ITCZ (Souza & Cavalcanti, 2009). This explains its high correlation with the Caribbean SLP.

The NAO is related to the Atlantic SST as shown by the first winter SST EOF analysis. However, its correlation with the Norwegian SST is weaker, but still positive and significant at interannual and decadal timescales. The NAO's correlation with Caribbean SST is also weak and only significant at interannual timescales. King & Kucharski (2006) performed a maximum covariance analyses (MCA) of the Hadley Centre SST data set that also indicated a negative correlation between the NAO and tropical Atlantic SST, with r values between -0.16 and -0.20 for regions just east of the Cariaco Basin. The MCA data also indicate that the influence of the NAO on tropical Atlantic SST weakens after 1960, what agrees with the anomalous SST positive trend in the late decades found in our results, and relates to the fact that the oceanic influence on North Atlantic climate is considered nonstationary at interannual scales (Sutton & Hodson, 2003). Black et al. (2007), comparing a Mg/Ca SST proxy record to the Hurrell (1995) NAO index, also found a weak but statistically significant correlation with same sign and magnitude

(r = -0.20) significant at the 95% level. This increased to -0.31 (99% level) if only years prior to 1960 were considered. Earlier analysis of instrumental records demonstrated that tropical Atlantic and Caribbean SST variability is correlated with the ENSO variability (Giannini et al., 2000), what may explain the weak correlations with the NAO only.

Stronger and more organized correlations between the SST indices and the AMO index at interannual and interdecadal scales seem to indicate that multidecadal variability in the ocean's thermohaline circulation may be an important component of the covariability between these two areas. While the interannual correlation maps between the Norwegian SST and SST elsewhere reflect a clear NAO imprint on SST, the decadal map resembles the AMO SST pattern (Fig. 4.11) (Sutton & Hodson, 2005). However, our results further show a surprising uncorrelated area south of Greenland, where important processes associated with the thermohaline circulation take place (Kushnir, 1994; Timmermann et al., 1998; Delworth & Greatbatch, 2000). This difference is interpreted as if the covariability of the Norwegian Sea SST at longer timescales is influence by processes other than only the MOC variability. Part of long term SST variability could be attributed to solar insolation, what could explain such wide distribution of positively correlated SST anomalies. Solar variability components related to the Gleissberg cycle (70-100 years) for instance, have been identified in other studies (Risebrobakken et al., 2003; Grosfeld et al., 2007).

The interannual relations between the Norwegian Sea SST and SLP fields elsewhere is similar to a dipole–like pattern. In these correlation maps, a persistent negative signal covers most of the Nordic Seas and a smaller positive area off Newfoundland is seen during wintertime and in the annual means, but not in the summer. In other words, in the presence of lower surface pressure in the Nordic Seas, a cyclonic circulation develops and positive SST anomalies occur in the Norwegian Sea, positively correlated with the mid latitudes anticyclonic circulation associated with higher SLP and positive SST anomalies (see Fig. 4.12 a-c). The positively correlated area off Newfoundland match the higher positive anomalies of SST described by Bjerknes (1964); Kushnir (1994); Timmermann et al. (1998) and Delworth & Greatbatch (2000). This is further associated with surface fluxes variations as a response to the atmospheric forcing of the NAO, although the positions are displaced from NAO's main centers of action (Icelandic Low and Azores High) and show comparatively reduced significative areas. This result therefore, indicates that over this region oceanic responses related to wind–evaporation processes are important for controlling the climate variability.

Moreover, this spatial pattern is also revealed at interdecadal timescales, likely associated with THC fluctuations (Delworth & Greatbatch, 2000) driven by an atmospheric pattern similar to the NAO (Latif et al., 2006) (Fig. 4.11d). The NAO and associated wind fields modify the surface ocean salinity and temperature which in turn affect the convection in the regions of deep-water formation, i.e. the Labrador, Irminger and Greenland seas, as well as sea ice dynamics (Marshall et al., 2001; Furevik & Nilsen, 2005; Sicre et al., 2008). In agreement, our results suggest that the ocean responses to the atmosphere at interannual and interdecadal scales are likely to result from the high and low frequency of a NAO–like atmospheric forcing, respectively.

The MOC variability has been linked to a low frequency atmospheric mode, and it has been reproduced in numerous modelling studies, although with different periodicity (Timmermann et al., 1998; Delworth & Greatbatch, 2000; Vellinga & Wu, 2004). In our results the signal over the Caribbean Sea could be related to the results of Sicre et al. (2008), who investigated a SST paleo reconstruction off North Iceland. They suggested that low frequency NAO forcing could be responsible for part of the variability of SST found in the record, but also related it to MOC oscillations induced by ENSO activity. The mechanism involves linkages between high latitude SST and the tropical ITCZ, as recorded by the Cariaco Basin sediments. For instance, freshwater export from the Atlantic to the Pacific during warm ENSO phases, would generate positive salinity anomalies in the tropical Atlantic. This leads to an anomalously strong THC and northward ocean transport that generates a cross–equatorial gradient where the North Atlantic is relatively warmer than the South Atlantic (Timmermann et al., 1998; Knight et al., 2005), and the ITCZ moves northward (Nobre & Shukla, 1996; Hastenrath, 2006). The rainfall associated with the ITCZ produces an anomalous freshwater flux and a salinity anomaly, which travels towards the pole at a lag of 5-6 decades. This low surface salinity anomalies slow down the THC, leading to the opposite phase (Vellinga & Wu, 2004). This slow traveling low density tropical anomalies have also been hypothesized by Bjerknes (1964), although due to the lack of measurements in the south and tropical Atlantic his work was not conclusive regarding this aspect. Figure 5.1 is the schematic representation of this mechanism.

Thus positive ENSO phases, will increase freshwater export from the Atlantic to the Pacific and generate salinity anomalies in the tropical Atlantic (Giannini et al., 2000), affecting high latitudes sinking regions and subsequently the MOC and the ITCZ dynamics (Sicre et al., 2008). Considering that the Atlantic and Pacific climate variability interact and can contribute to positive or negative interferences, the ENSO effects should not be ignored (Giannini et al., 2000; Hoerling et al., 2001). For instance, the Pacific–North American (PNA) teleconnection pattern, with a centre of action off Newfoundland, interferes with the strength of trade winds in the North Atlantic and the position of SLP anomalies in the Atlantic (Timmermann et al., 1998; Giannini et al., 2000). It too may be related to the center seen in the correlation map between Norwegian SST and SLP, at interannual and decadal scales.

Other modelling studies that considered the shutdown of the THC due to freshwater input to the high latitudes predicted a southward shift of the ITCZ, associated to a colder North Atlantic, leading to the chain of consequences in rainfall pattern over the tropics (Broecker, 2003). Otterå et al. (2004), who performed simulations with the Bergen climate model, described a cycle where an atmospheric–sea–ice–ocean NAO–like response occurs to enhanced freshwater input to the Nordic and Arctic Seas. Yang (1999) have also shown statistically significant cross-correlation between Labrador Sea Water thickness and tropical SST dipole, suggesting a linkage with the MOC, likely to respond to both the NAO and the Arctic freshwater input. Differences in such relations compared to our results might arise from the use of different areas, since the Norwegian Sea is connected by the overflow to the sinking zones, but is not itself an important convective region. Instead, it responds directly to the atmospheric forcing associated with the NAO and

its impact over the North Atlantic Water (NAW) (Furevik & Nilsen, 2005). Although Delworth & Greatbatch (2000) conclude that the heat flux in the North Atlantic is dominant in relation to freshwater and momentum fluxes in driving the THC variability, air–sea coupling appears to modify the amplitude of the variability.

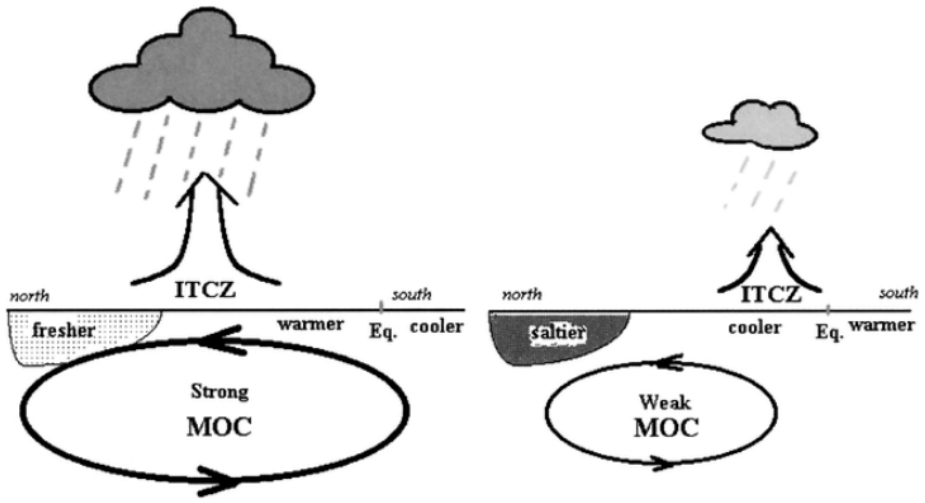

Figure 5.1: Proposed mechanism for centennial THC fluctuation. When the MOC is strong (left) the ITCZ shifts northward, in response to enhanced SST gradient across the equator, where the North Atlantic is relatively warmer to the South Atlantic. Freshwater anomalies travel in the ocean surface northward and weaken the overturning, leading to a reverse phase (right). According to Hastenrath (2006) the ITCZ would be located further to the south, explaining the positive rainfall anomalies in the Nordeste simultaneously to dry conditions, enhanced trade winds and upwelling intensity in the Cariaco Basin (Black et al., 1999). From Vellinga & Wu (2004); their Figure 16.

Evidence from paleo records support the hypothesis that changes in the MOC, herein represented by the AMO index, are synchronized with covariability in the North Atlantic and the tropical Caribbean Sea. Cold episodes during the last glacial periods involved changes in the thermohaline circulation, with reduced or absent heat transport from the tropics, associated with intense cooling in high latitudes. Shifts in the intensity and location of atmospheric convection and rainfall, including the Atlantic ITCZ, in turn affected the salinity and density of surface waters, which are decisive to the strength of the THC (Chiang & Koutavas, 2004).

Using a sensitivity model, Chiang et al. (2003) investigated how the Atlantic ITCZ responded to the cooling occurred during the Last Glacial Maximum, and its connections with land ice sheet, thermohaline ocean transport, and sea ice. Their results show that a meridional mode and an ITCZ response (similar to the modern interannual – decadal variability) changed concurrent to land ice, forcing a cooling of the north tropical Atlantic SST, enhancing northern trade winds and displacing the ITCZ southward. However, they also comment, without being conclusive, that mechanisms associated with heat transport through THC, and sea ice cover have impact on the meridional mode and the ITCZ position through other means, other than the trade wind variations.

In summary, a "thermohaline reorganization" explains the synchronous changes in the oceanic heat transport and circulation, strength of the MOC, the meridional mode of SST gradient in the tropical Atlantic and the ITCZ position, consistent with the registered covariability patterns of the high latitudes and the tropics at different timescales (Black et al., 1999; Hughen et al., 2000; Peterson & Haug, 2006). The atmospheric related mechanism points to a NAO–like pattern that at interannual to decadal scales drive changes and feedback between the air–sea heat fluxes as a result of anomalous surface wind, Ekman transport and thermodynamic processes (Bjerknes, 1964; Kushnir, 1994; Giannini et al., 2000; George & Saunders, 2001; Marshall et al., 2001; Czaja & Frankignoul, 2002; Hurrell et al., 2006).

Chapter 6

Summary and concluding remarks

Motivated by the covariability of paleorecords from Norwegian Sea and Cariaco Basin, this thesis explored instrumental SST and SLP data in both areas, at interannual and interdecadal timescales and covered the years from 1856 to 2008. Relationships with the NAO and AMO were investigated in search of possible mechanisms driving such connections.

Following the three key questions raised in the introduction, the main findings are:

1. Interannual covariability between the Norwegian Sea SST and the Caribbean Sea SST and SLP is weak, compared to interdecadal correlations. At interannual and interdecadal scales both the SST and the SLP patterns are coherent to responses to a NAO–like forcing, even if the NAO alone does not explain much of the covariability between the indices. The correlation between the Norwegian SST and the North Atlantic SLP field suggests that the tropical western Atlantic responds to external forcing other than the NAO, such as the ENSO or the PNA. At interdecadal timescales the SST correlation map is similar to the spatial pattern of the AMO, except for the area south of Greenland, where changes in the MOC seem to be in part independent from processes driving the Norwegian Sea SST variability. Thus, the climate variability in the North Atlantic at interannual and interdecadal timescales can be mostly explained by, respectively, local oceanic heat, and oceanic circulation responses to anomalies in the atmospheric forcing, as extensively described in the literature (Bjerknes, 1964; Kushnir, 1994; Timmermann et al., 1998; Delworth & Greatbatch, 2000).

2. Interdecadal covariability of the ITCZ position and the North Atlantic high latitude climate seems to arise from low frequency atmospheric variability related to MOC variability. The mechanism involves changes in high latitude ocean density and rainfall dynamics in the tropical Atlantic, connected to SST and surface salinity anomalies transported northward affecting the strength of the THC and the cross–equatorial SST (Vellinga & Wu, 2004; Sicre et al., 2008).

3. This mechanism is also one likely explanation for the past climate teleconnections, considering the respective differences in geographical extension and timescales associated with prolongated and abrupt climatic events such as the Little Ice Age and the Younger Dryas.

Despite the suggestive correlations, it is not possible to determine the origin and nature of

the forcing of the covariability between Atlantic high latitudes and the tropical Atlantic based on our two SST and SLP data sets. For a more complete investigation of the relationships discussed in this study, a suite of fully coupled climate models should be analyzed.

Bibliography

Alley, R. B., Marotzke, J., Nordhaus, W. D., Overpeck, J. T., Peteet, D. M., Pielke, R. A. J., Pierrehumbert, R. T., Rhines, P. B., Stocker, T. F., Talley, L. D., & Wallace, J. M. (2003). Abrupt climate change. *Science*, *299*(5615), 2005–2010.

Baker, P. (2002). Trans-Atlantic climate connections. *Science*, *296*(5565), 67–68.

Baker, P., Rigsby, C., Seltzer, G., Fritz, S., Lowenstein, T., Bacher, N., & Veliz, C. (2001). Tropical climate changes at millennial and orbital timescales on the Bolivian Altiplano. *Nature*, *409*(6821), 698–701.

Bjerknes, J. (1964). Atlantic air–sea interaction. *Advances in Geophysics. Academic Press*, *10*, 1–82.

Black, D., Peterson, L., Overpeck, J., Kaplan, A., Evans, M., & Kashgarian, M. (1999). Eight centuries of North Atlantic Ocean atmosphere variability. *Science*, *286*(5445), 1709–1713.

Black, D. E., Abahazi, M. A., Thunell, R. C., Kaplan, A., Tappa, E. J., & Peterson, L. C. (2007). An 8-century tropical atlantic SST record from the Cariaco Basin: Baseline variability, twentieth-century warming, and Atlantic hurricane frequency. *Paleoceanography*, *22*(4).

Broecker, W. (2003). Does the trigger for abrupt climate change reside in the ocean or in the atmosphere? *Science*, *300*(5625), 1519–1522.

Calvo, E., Grimalt, J., & Jansen, E. (2002). High resolution U_{37}^K sea surface temperature reconstruction in the Norwegian Sea during the Holocene. *Quaternary Science Reviews*, *21*(12-13), 1385–1394.

Chiang, J., Biasutti, M., & Battisti, D. (2003). Sensitivity of the Atlantic Intertropical Convergence Zone to Last Glacial Maximum boundary conditions. *Paleoceanography*, *18*(4).

Chiang, J., & Koutavas, A. (2004). Tropical flip-flop connections. *Nature*, *432*(7018), 684–685.

Chiang, J., Kushnir, Y., & Giannini, A. (2002). Deconstructing Atlantic Intertropical Convergence Zone variability: Influence of the local cross-equatorial sea surface temperature gradient and remote forcing from the eastern equatorial Pacific. *Journal of Geophysical Research-Atmospheres*, *107*(D1-D2).

Czaja, A., & Frankignoul, C. (2002). Observed impact of Atlantic SST anomalies on the North Atlantic Oscillation. *Journal of Climate*, *15*(6), 606–623.

Delworth, T., & Greatbatch, R. (2000). Multidecadal thermohaline circulation variability driven by atmospheric surface flux forcing. *Journal of Climate*, *13*(9), 1481–1495.

Emery, W. J., & Thomson, R. E. (2001). *Data Analysis Methods in Physical Oceanography*. Amsterdam, The Netherlands: Elsevier B.V., Second and revised ed.

Felis, T., Patzold, J., Loya, Y., Fine, M., Nawar, A., & Wefer, G. (2000). A coral oxygen isotope record from the northern Red Sea documenting NAO, ENSO, and North Pacific teleconnections on Middle East climate variability since the year 1750. *Paleoceanography*, *15*(6), 679–694.

Folland, C., Palmer, T., & Parker, D. (1986). Sahel rainfall and worldwide sea temperature, 1901-85. *Nature*, *320*(6063), 602–607.

Furevik, T., & Nilsen, J. E. Ø. (2005). *Large-Scale Atmospheric Circulation Variability and its Impacts on the Nordic Seas Ocean Climate - a Review*. 158. AGU, Geophysical Monograph Series.

George, S., & Saunders, M. (2001). North Atlantic Oscillation impact on tropical north Atlantic winter atmospheric variability. *Geophysical Research Letters*, *28*(6), 1015–1018.

Giannini, A., Kushnir, Y., & Cane, M. (2000). Interannual variability of Caribbean rainfall, ENSO, and the Atlantic Ocean. *Journal of Climate*, *13*(2), 297–311.

Glantz, M. H., Katz, R. W., & Nicholls, N. (Eds.) (1991). *Teleconnections linking worldwide climate anomalies: scientific basis and societal impact*. Cambridge University Press.

Grosfeld, K., Lohmann, G., Rimbu, N., Fraedrich, K., & Lunkeit, F. (2007). Atmospheric multidecadal variations in the North Atlantic realm: proxy data, observations, and atmospheric circulation model studies. *Climate of the Past*, *3*(1), 39–50.

Hannachi, A., Jolliffe, I. T., & Stephenson, D. B. (2007). Empirical orthogonal functions and related techniques in atmospheric science: A review. *International Journal of Climatology*, *27*(9), 1119–1152.

Hastenrath, S. (2006). Circulation and teleconnection mechanisms of Northeast Brazil droughts. *Progress In Oceanography*, *70*(2-4), 407–415.

Haug, G., Hughen, K., Sigman, D., Peterson, L., & Rohl, U. (2001). Southward migration of the Intertropical Convergence Zone through the Holocene. *Science*, *293*(5533), 1304–1308.

Hoerling, M., Hurrell, J., & Xu, T. (2001). Tropical origins for recent North Atlantic climate change. *Science*, *292*(5514), 90–92.

Hughen, K., Southon, J., Lehman, S., & Overpeck, J. (2000). Synchronous radiocarbon and climate shifts during the last deglaciation. *Science*, *290*(5498), 1951–1954.

Hurrell, J. (1995). Decadal trends in the North Atlantic Oscillation: Regional temperatures and precipitation. *Science*, *269*(5224), 676–679.

Hurrell, J. W., Visbeck, M., Busalacchi, A., Clarke, R. A., Delworth, T. L., Dickson, R. R., Johns, W. E., Koltermann, K. P., Kushnir, Y., Marshall, D., Mauritzen, C., McCartney, M. S., Piola, A., Reason, C., Reverdin, G., Schott, F., Sutton, R., Wainer, I., & Wright, D. (2006). Atlantic climate variability and predictability: A CLIVAR perspective. Journal of Climate.

Johnson, T., Brown, E., McManus, J., Barry, S., Barker, P., & Gasse, F. (2002). A high-resolution paleoclimate record spanning the past 25,000 years in southern East Africa. *Science*, *296*(5565), 113–116.

Kalnay, E., Kanamitsu, M., Kistler, R., Collins, W., Deaven, D., Gandin, L., Iredell, M., Saha, S., White, G., Woollen, J., Zhu, Y., Chelliah, M., Ebisuzaki, W., Higgins, W., Janowiak, J., Mo, K., Ropelewski, C., Wang, J., Leetmaa, A., Reynolds, R., Jenne, R., & Joseph, D. (1996). The NCEP/NCAR 40-year reanalysis project. *Bulletin of the American Meteorological Society*, *77*(3), 437–471.

Kaplan, A., Cane, M., Kushnir, Y., Clement, A., Blumenthal, M., & Rajagopalan, B. (1998). Analyses of global sea surface temperature 1856-1991. *Journal of Geophysical Research-Oceans*, *103*(C9), 18567–18589.

King, M., & Kucharski, F. (2006). Observed low-frequency covariabilities between the tropical oceans and the North Atlantic Oscillation in the twentieth century. *Journal of Climate*, *19*(6), 1032–1041.

Knight, J., Allan, R., Folland, C., Vellinga, M., & Mann, M. (2005). A signature of persistent natural thermohaline circulation cycles in observed climate. *Geophysical Research Letters*, *32*(20).

Knight, J. R., Folland, C. K., & Scaife, A. A. (2006). Climate impacts of the Atlantic Multidecadal Oscillation. *Geophysical Research Letters*, *33*(17).

Kushnir, Y. (1994). Interdecadal variations in North Atlantic sea surface temperature and associated atmospheric conditions. *Journal of Climate*, *7*(1), 141–157.

Latif, M., Boening, C., Willebrand, J., Biastoch, A., Dengg, J., Keenlyside, N., Schweckendiek, U., & Madec, G. (2006). Is the thermohaline circulation changing? *Journal of Climate*, *19*(18), 4631–4637.

Lea, D., Pak, D., Peterson, L., & Hughen, K. (2003). Synchroneity of tropical and high-latitude Atlantic temperatures over the last glacial termination. *Science*, *301*(5638), 1361–1364.

Ledru, M., Mourguiart, P., Ceccantini, G., Turcq, B., & Sifeddine, A. (2002). Tropical climates in the game of two hemispheres revealed by abrupt climatic change. *Geology*, *30*(3), 275–278.

Liu, Z., & Alexander, M. (2007). Atmospheric bridge, oceanic tunnel, and global climatic teleconnections. *Reviews of Geophysics*, *45*(2).

Marshall, J., Kushnir, Y., Battisti, D., Chang, P., Czaja, A., Dickson, R., Hurrell, J., McCartney, M., Saravanan, R., & Visbeck, M. (2001). North Atlantic climate variability: Phenomena, impacts and mechanisms. *International Journal of Climatology*, *21*(15), 1863–1898.

Mauritzen, C., Hjollo, S. S., & Sando, A. B. (2006). Passive tracers and active dynamics: A model study of hydrography and circulation in the northern North Atlantic. *Journal of Geophysical Research-Oceans*, *111*(C8).

Nobre, P., & Shukla, J. (1996). Variations of sea surface temperature, wind stress, and rainfall over the tropical Atlantic and South America. *Journal of Climate*, *9*(10), 2464–2479.

Otterå, O., Drange, H., Bentsen, M., Kvamstø, N., & Jiang, D. (2004). Transient response of the Atlantic meridional overturning circulation to enhanced freshwater input to the Nordic Seas–Arctic Ocean in the Bergen climate model. *Tellus Series A-Dynamic Meteorology and Oceanography*, *56*(4), 342–361.

Peterson, L., & Haug, G. (2006). Variability in the mean latitude of the Atlantic Intertropical Convergence Zone as recorded by riverine input of sediments to the Cariaco Basin (Venezuela). *Palaeogeography, Palaeoclimatology, Palaeoecology*, *234*(1), 97–113.

Quenouille, M. H. (1952). *Associated measurements*. London: Butterworths.

Risebrobakken, B., Jansen, E., Andersson, C., Mjelde, E., & Hevroy, K. (2003). A high-resolution study of Holocene paleoclimatic and paleoceanographic changes in the Nordic Seas. *Paleoceanography*, *18*(1).

Rodwell, M., Rowell, D., & Folland, C. (1999). Oceanic forcing of the wintertime North Atlantic Oscillation and European climate. *Nature*, *398*(6725), 320–323.

Ruiz-Barradas, A., Carton, J., & Nigam, S. (2000). Structure of interannual-to-decadal climate variability in the tropical Atlantic sector. *Journal of Climate*, *13*(18), 3285–3297.

Sicre, M.-A., Yiou, P., Eiriksson, J., Ezat, U., Guimbaut, E., Dahhaoui, I., Knudsen, K.-L., Jansen, E., & Turon, J.-L. (2008). A 4500-year reconstruction of sea surface temperature variability at decadal time-scales off North Iceland. *Quaternary Science Reviews*, *27*(21-22), 2041–2047.

Souza, P., & Cavalcanti, I. F. A. (2009). Atmospheric centres of action associated with the Atlantic ITCZ position. *International Journal of Climatology*, (DOI: 10.1002/joc).

Stocker, T. (2003). South dials north. *Nature*, *424*(6948), 496–499.

Sutton, R., & Hodson, D. (2003). Influence of the ocean on North Atlantic climate variability 1871-1999. *Journal of Climate*, *16*(20), 3296–3313.

Sutton, R., & Hodson, D. (2005). Atlantic Ocean forcing of North American and European summer climate. *Science*, *309*(5731), 115–118.

Sutton, R. T., & Hodson, D. L. R. (2007). Climate response to basin-scale warming and cooling of the North Atlantic Ocean. *Journal of Climate*, *20*(5), 891–907.

Timmermann, A., Latif, M., Voss, R., & Grotzner, A. (1998). Northern Hemispheric interdecadal variability: A coupled air-sea mode. *Journal of Climate*, *11*(8), 1906–1931.

Vellinga, M., & Wu, P. (2004). Low-latitude freshwater influence on centennial variability of the Atlantic thermohaline circulation. *Journal of Climate*, *17*(23), 4498–4511.

Wang, X., Auler, A., Edwards, R., Cheng, H., Cristalli, P., Smart, P., Richards, D., & Shen, C. (2004). Wet periods in northeastern Brazil over the past 210 kyr linked to distant climate anomalies. *Nature*, *432*(7018), 740–743.

Woodruff, S., Slutz, R., Jenne, R., & Steurer, P. (1987). A comprehensive ocean-atmosphere data set. *Bulletin of the American Meteorological Society*, (68), 1239–1250.

Wu, L., & Liu, Z. (2002). Is Tropical Atlantic Variability driven by the North Atlantic Oscillation? *Geophysical Research Letters*, *29*(13).

Xie, S., & Carton, J. (2004). Tropical Atlantic Variability: Patterns, mechanisms, and impacts. In C. Wang, S. Xie, & J. Carton (Eds.) *Earth Climate: the ocean–atmosphere interaction*, vol. 147 of *Geophysical Monographs*, (pp. 121–142). American Geophysical Union, AGU.

Yang, J. (1999). A linkage between decadal climate variations in the Labrador Sea and the tropical Atlantic Ocean. *Geophysical Research Letters*, *26*(8), 1023–1026.